Lipid homeostasis is essential for endoplasmic reticulum protein quality control

By

Gilberto Garcia

A dissertation submitted in partial satisfaction of the

Requirements for the degree of

Doctor of Philosophy

in

Molecular and Cell Biology

in the

Graduate Division

of the

University of California, Berkeley

Committee in charge:

Professor Andrew George Dillin, Chair
Professor Abby Dernburg
Assistant Professor Roberto Zoncu
Associate Professor James Olzmann

Summer 2019

Abstract

Lipid homeostasis is essential for endoplasmic reticulum protein quality control

By

Gilberto Garcia
Doctor of Philosophy in Molecular and Cell Biology
University of California, Berkeley
Professor Andrew George Dillin, Chair

The endoplasmic reticulum (ER) is a critical organelle for protein synthesis, protein trafficking, and lipid synthesis. As such, cells have evolved a quality control system known as the ER Unfolded Protein Response (UPR^{ER}). Capable of monitoring protein folding and membrane lipid composition to preserve ER homeostasis, the UPR^{ER} is crucial for responding to cellular stress brought on by increased metabolic demand, environmental factors, and aging. In this study, we have identified *let-767* as an essential gene for ER homeostasis. Through an RNAi screen of lipid droplet associated genes, we found that knockdown of *let-767* resulted in reduced lipid droplets, aberrant ER morphology, and compromised UPR^{ER} induction, which impacted growth and lifespan. We found that these deficiencies in ER quality were independent of *let-767*'s previously characterized function in mono-methyl branched chain fatty acid synthesis (mmBCFAs), as supplementation of mmBCFAs did not ameliorate the detrimental phenotypes. However, supplementation of whole animal lysate was able to rescue the lipid droplet depletion, ER morphology, and animal growth, but not the UPR^{ER} function. The UPR^{ER} induction was instead rescued by reducing the *let-767* pathway through knockdown of the upstream transcription factor *sbp-1*, suggesting accumulation of a potential toxic metabolite within the *let-767* pathway. Our results indicate that *let-767* may play a more significant role in lipid metabolism than has been previously described and highlight the importance of lipid homeostasis to protein quality control.

Table of Contents

Acknowledgements

First and foremost, I would like to thank my advisor, Professor Andrew George Dillin, for the patience and independence to follow my scientific curiosities in his lab. It's been a learning experience both scientifically and personally. I would also like to thank the rest of my thesis committee, Professor Abby Dernburg, Professor Roberto Zoncu, and Professor James Olzmann for their helpful comments and advice. Additionally, I would like to thank Professor Abby Dernburg for the use of her spinning disk microscope that was used in this study.

I would like to thank everyone in Dillin lab for countless useful scientific conversations that helped make this dissertation possible. I especially want to thank Dr. Joseph R. Daniele for his perfectly cromulent help in starting my project, Dr. Ryo Higuchi-Sanabria for his guidance in my scientific career and this dissertation, and Dr. Brant M. Webster for his scientific insight and words.

Lastly, I would like to thank my family and friends for their support during all these years of education, especially my sister and brother-in-law. You two have been a continuous source of support and joy during my time in graduate school.

Chapter 1: Introduction

1.1 Cellular Proteostasis and the Endoplasmic Reticulum

Proteins function in every aspect of the cell, from structural support to carrying out complex enzymatic reactions. As such, monitoring and preserving protein quality is vital for cellular function. Stable maintenance of proteins and protein complexes in a properly folded and assembled state while balancing protein synthesis and turnover is collectively known as protein homeostasis, or proteostasis [1]. Central to maintaining this balanced state are chaperones, proteins capable of folding and unfolding cellular proteins or binding them to prevent aggregation and promoting their clearance [2]. Due to the unpredictable nature of life, cells must also be capable of responding to numerous environmental and biological stresses to maintain proteostasis and preserve cellular function.

Within eukaryotic cells, membrane bound organelles carry out specialized tasks requiring distinct local environments, adding to the intricacy of maintaining proteostasis. To this end, cells have evolved compartment specific systems capable of responding to perturbations in proteostasis within the cytoplasmic, mitochondrial, and endoplasmic reticulum (ER) compartments. These stress response systems are known as the heat shock response (HSR), mitochondrial unfolded protein response (UPR^{mito}), and the endoplasmic reticulum unfolded protein response (UPR^{ER}), respectively. Upon activation, these systems initiate complex genetic programs via key transcription factors: *hsf-1* (HSF1, mammalian ortholog), *atfs-1* (ATF4, mammalian ortholog), and *xbp-1* (XBP1, mammalian ortholog), respectively. While all three of these genetic programs commonly result in upregulation of chaperones to manage protein quality, each stress response also alters compartment specific factors to preserve organelle function [3].

Of the three major unfolded protein responses, the UPR^{ER} possesses the most branched input mechanism. To maintain proteostasis of the ER, the UPR^{ER} incorporates 3 distinct signaling transmembrane proteins into its activation: PEK-1 (PERK, human ortholog), ATF-6 (ATF6, human ortholog), and IRE-1 (IRE1, human ortholog). Within the ER lumen, these proteins are bound by the HSP70 chaperone, HSP-4 (HSP5A/BiP, human ortholog), under basal conditions. Upon protein misfolding, HSP-4 is titrated away from them to allow the luminal domains of IRE-1 and PEK-1 to interact with misfolded proteins, which induce dimerization and activation through transphosphorylation of cytosolic kinase domains. The activated PEK-1 is then able to phosphorylate the translation initiation factor EIF2a (EIF2A, human ortholog) to globally reduce translation and preferentially translate the transcription factor ATF-5 (ATF4, human ortholog) to initiate its stress response. Upon IRE-1's activation, the cytosolic RNAse domain begins splicing *xbp-1* mRNA to the much more active *xbp-1s* isoform, launching its genetic program. IRE-1's activation also results in its oligomerization which promotes regulated IRE1-dependent decay of mRNA (RIDD) to further reduce the ER protein load [4]. Uniquely, ATF-6 does not oligomerize upon HSP-4 dissociation, but instead is trafficked to the Golgi complex where it is cleaved from the membrane and imported into the nucleus to induce expression of stress response genes [5].

Together, these three sensors and their corresponding transcription factors are responsible for maintaining the ER proteostasis and determining a cell's fate. When proteostasis cannot be

maintained, prolonged activation of the UPR^{ER} can lead to apoptosis, inflammatory signaling, or accumulation of toxic protein species, resulting in impeded cellular function and disease. This association between impaired proteostasis and compromised health has been observed in numerous chronic conditions, including diabetes, aging, and especially neurodegenerative disease. In the case of neurodegenerative disorders, affected individuals exhibit hallmark neurological symptoms, but also present with pathological accumulations of intracellular and/or extracellular protein aggregates [6]–[8]. Interestingly, these symptoms usually appear later in the individual's life, which coincides with an organism's increasingly dysfunctional UPR^{ER} [9], [10]. Whether these aggregates contribute to the disease progression or are merely a symptom of global loss of proteostasis is not fully understood [11]. However, ectopic manipulation of the stress response pathways has been observed to increase protection from proteotoxic stress and increase the median lifespan of model organisms [12]–[14]. As such, these stress pathways are very active areas of study with the goal of elucidating unknown factors which regulate or influence the regenerative potential of the HSR, UPR^{mito}, and UPR^{ER}.

1.2 Lipid homeostasis and the endoplasmic reticulum

Much like proteins, lipids play multiple roles within a cell, from being the key component in membranes to functioning as signaling or energy storage molecules. These macromolecules exist in highly variable molecular structures that can be joined together or modified to form more complex lipids with distinct signaling and physical properties from their simpler counterparts. It is therefore vital that lipid quantity and composition be monitored to preserve lipid homeostasis and prevent lipotoxic accumulation of lipid metabolites.

Fatty acids and cholesterol are fundamental lipids and integral to membrane quality. As components of multiple lipid subtypes such as phospholipids and sphingolipids, fatty acid chain lengths, attached head groups, and branched or saturated characteristics can have significant effects on membrane dynamics, thickness, and curvature. Additionally, the breakdown of these more complex lipid species to diacylglycerol or ceramide, respectively, not only affect membrane quality, but also function as strong signaling molecules which can have dramatic effects if their quantity is not regulated. Similarly, cholesterol and its metabolites have significant effects on membrane fluidity while also serving as precursors for powerful signaling molecules known as steroid hormones [15], [16]. To prevent the toxic accumulation of these bioactive lipid species, cells can convert sterols and fatty acids into cholesteryl esters, triglycerides, or other neutral lipids [17], [18]. These highly hydrophobic molecules lack charged groups, making them inert and the preferred lipid storage form of cells.

Lipids are processed within multiple compartments of a cell; however, specific organelles play distinct roles in lipid metabolism. Initial fatty acid synthesis mainly occurs within the mitochondria and cytoplasm. These fatty acids are then elongated by the mitochondria, cytoplasm, and ER [19], [20]. Mitochondria are also a site of fatty acids catabolism. Mitochondria break down fatty acids through beta-oxidation with peroxisomes, which also perform alpha-oxidation of branched fatty acids. While peroxisomes can also synthesize complex ether lipids, most other lipids such as membrane lipids, cholesterol, and neutral lipids are

synthesized by the ER, making the ER a major site of lipid metabolism[21], [22]. As such, the ER is a primary source of membrane lipids for multiple organelles.

Basal lipid metabolism is largely maintained through ligand-activated control of transcription factors which regulate multiple enzymes of lipogenic pathways [23]. One such transcription factor, the Sterol Regulatory Element-Binding Protein (SREBP), is localized to the ER. SREBP is highly conserved from yeast (Mga2 & Sre1) to mammals (SREBP1 & SREBP2) and incorporates numerous metabolic cues from insulin, mammalian target of rapamycin (mTOR), and downstream lipid products. Similar to ATF6, SREBP activation is dependent on its trafficking to the Golgi complex, where it is proteolytically processed and freed to enter the nucleus. Once activated, SREBP functions with multiple cofactors to control a variety of lipid pathways including cholesterol, fatty acid, and complex lipid synthesis [24].

As a crucial organelle to lipid homeostasis, the ER has evolved lipid homeostasis sensors. Interestingly, these sensors are also the UPR^{ER} transmembrane proteins, IRE1, PERK, and ATF6. Adjacent to their transmembrane helices, IRE1 and PEK1 contain an amphipathic helix capable of sensing general ER membrane imbalances and activating the UPR^{ER} independent of their luminal unfolded protein sensing domains [25], [26]. Within the transmembrane domain of ATF6, a sphingolipid sensing motif triggers ATF6 activation upon accumulation of dihydrosphingosine or dihydroceramide, also independent of proteotoxic stress [27]. In combination with basal lipid metabolism transcription factors, these proteins play an integral role in maintaining lipid homeostasis.

Utilizing the same stress response sensors for protein and lipid stress results in an undeniable link between lipid and ER protein homeostasis. This association is highlighted in individuals suffering from obesity. Aside from aberrant lipid storage and regulation, these individuals also present with systemic inflammation, a known symptom of chronic ER stress [28], [29]. Conversely, ER stress within the brain's metabolic control center, the hypothalamus, has been shown to contribute to metabolic changes that instigate weight gain and insulin resistance in mice, hallmark symptoms of obesity [9], [30]. These associations suggest that the UPR^{ER} likely plays a role in the mechanism of lipotoxicity. Interestingly, individuals in advanced age, with likely compromised UPR^{ER} activity, also present with many conditions associated with obesity, suggesting that UPR^{ER} is also crucial for maintaining lipid homeostasis [31].

1.3 Lipid droplets and lipid homeostasis

Conserved from bacteria to humans, lipid droplets are integral to lipid homeostasis. They store neutral lipids within a core surrounded by a phospholipid monolayer decorated with regulatory and enzymatic proteins. Within eukaryotes, lipid droplets are formed through deposition of neutral lipids between the ER membrane leaflets. After stabilization of these deposits by various proteins, further deposition of neutral lipids allows for growth and eventual release of a mature lipid droplet into the cytosol. Ranging in size from a few nanometers to 200 μm within multiple cell types, they function as dynamic hubs for sequestering bioactive molecules as neutral lipids, while also providing a means to regulate lipid distribution and surplus lipids to maintain lipid homeostasis [17], [32].

Once thought to be inert vesicles of lipids, lipid droplets are now understood to play an active role in regulating lipid homeostasis and influencing metabolism. Both enzymatic and regulatory proteins are targeted to lipid droplets during their biogenesis and contribute to their growth and dynamic characteristics. Acyltransferases allow for triglyceride synthesis and cholesterol esterification, while lipases and hydrolases can mobilize neutral lipids into their active metabolites [17]. Of the lipid droplet regulatory proteins, the perilipin family is the best characterized. They function in stabilization of lipid droplets during biogenesis and regulate lipolysis. Under basal conditions, Perilipin 1 limits lipolysis by binding to Comparative Gene Identification 58 (CGI-58) to prevent both proteins from associating with lipases. Activation of Perilipin 1 through phosphorylation results in its dissociation from CGI-58 and each protein's association with Adipose Triglyceride Lipase (ATGL) and Hormone Sensitive Lipase (HSL), respectively, inducing a >50-fold increase in lipolysis [33]. To further regulate the cellular lipid pool, cells preferentially funnel lipids through lipid droplets instead of directly to various organelles, likely serving as a safeguard against transiently excessive or limiting pools of intracellular lipids. The direct interaction between lipid droplets and other organelles then allows for improved control over local transfer of lipids during times of need [34], [35]. This interaction can also serve as a metabolic cue. In the case of mitochondria, associating with lipid droplets results in a metabolic shift distinct from that of unassociated mitochondria [36].

An inability to maintain lipid homeostasis results in aberrant lipid accumulation and impaired cellular function. These effects are clearly observed in cases of lipodystrophies and obesity. Due to congenital defects in lipid storage genes or drug treatments (e.g. antiretroviral therapy), individuals with lipodystrophies are unable to effectively store lipids within their adipose tissue, cells highly enriched with lipid droplets to specifically store excess lipids. This results in aberrant lipid accumulation and often leads to the development of diabetes, hypertriglyceridemia, pancreatitis, and hepatic steatosis [37]. Conversely, individuals with obesity can store lipids within their adipose tissue but are unable to completely meet the demand due to the excessive consumption of lipids. This also results in an ectopic accumulation of lipids and development of diabetes, hypertriglyceridemia, and hepatic steatosis, as well as increased risks for heart disease, strokes, and kidney disease [38]–[40]. Interestingly, individuals with increased age are also at increased risk for these diseases, suggesting a general decline in lipid homeostasis with age [31].

As the central organelle for lipid storage, lipid droplet quality is crucial to maintaining lipid homeostasis. Expectedly, lipid droplets of obese individuals appear to be compromised in regulation and associations. Obese animals have reduced Perilipin 1 on adipose lipid droplets, thereby reducing effective control over lipolysis [41]. Within the muscle cells of obese individuals, the interaction between lipid droplets and mitochondria are impaired, likely leading to ineffective lipid transfer and altered metabolism [42]. Both instances would result in increased cellular lipids and possibly lipotoxic effects. In situations of excessive lipids, cells have been shown to efflux these bioactive molecules [34]. This increased circulation of lipids would then contribute to the aberrant lipid accumulation within uncommon cell types such as macrophages and hepatocytes, which are associated with disease states (i.e. atherosclerosis and hepatic steatosis) [43], [44]. While studies on obesity have been focused on inflammation, endocrine signaling, and organismal lipid accumulation, further understanding of how lipid droplets

properly store and regulate lipids may provide important insights on the roles that they play in metabolic disorders.

1.4 Non-canonical roles of lipid droplets

Lipid droplets have a highly dynamic range of size, unique structure, and intrinsic supply of lipid substrates. Cells have taken advantage of these characteristics and utilized lipid droplets for cellular functions beyond lipid storage. While all non-canonical functions are not known, their potential roles are hinted at by the diversity of lipid droplet associated proteins revealed in proteomic studies [45], [46].

The lipid droplet's cytoplasmic surface provides a unique surface for unconventional protein interactions. Drosophila embryos have taken advantage of this surface by utilizing it as a dynamic protein depot. Maternally deposited histones are stored on the lipid droplet surface through association with the lipid droplet protein Jabba. This association limits the degradation and toxic effects of free histones while allowing for their trafficking to nuclei as they are needed for embryo development. The surplus of histones also serves the secondary purpose of protecting the embryo from intracellular bacterial infections [46]. Yeast on the other hand, have been observed to utilize the lipid droplet surface as a protein carrier. The hydrophobic core and hydrophilic exterior allow effective association with unfolded ER proteins and their trafficking across the cytosol for degradation in the vacuole [47].

As the main lipid storage organelle, lipid droplets are poised to react to metabolic cues and alter their size and composition. Through changes in surface properties, lipid droplets are able to recruit or evict proteins, enabling cells to utilize these metabolic responses as a means of protein regulation. Bacterial lipid droplets have been observed to interact with genomic DNA under conditions of nutritional or UV stress. This association in turn, alters transcription and stabilizes DNA to promote survival [48]. Within adipocytes, the lipid droplet protein, Fsp27, associates with the transcription factor, Nfat5, sequestering it from the nucleus [49]. Changes in lipid metabolism leading to the dissociation of Fsp27 would then allow Nfat5 to enter the nucleus and induce its target gene expression.

The lipid droplet's ability to quickly store or mobilize resources enable the cell to effectively respond in situations of cellular stress. Upon nutrient deprivation for example, lipid droplets mobilize lipids to provide energy, but are also capable of limiting their utilization under extended periods of starvation to promote long term survival [50], [51]. This active control over lipid stores can also serve a protective role in situations of oxidative stress. By upregulating deposition of essential sensitive lipids such as polyunsaturated fatty acids, glial cells of developing *Drosophila* can limit oxidation of these molecules and preserve membrane quality and cellular function of neural stem cells [52]. However, it has been observed that accumulation of peroxidized lipids within glia, as a result of neuronal mitochondrial dysfunction, can precede neurodegeneration [53]. Whether the differences in developmental stage or mitochondrial function are the cause of these two contrasting outcomes is unknown, however, the formation of lipid droplets remains a clear response to oxidative stress.

Lipid droplets are also able to utilize their lipid stores in non-canonical ways. Clearance of specific inclusion bodies has been shown to be dependent on mobilization of lipid droplet sterol-metabolites. These sterols are likely used for production of chemical chaperones such as bile acids, sterol-based amphipathic molecules utilized for solubilization of nutrients during digestion [54]. It is evident that lipid droplets play many critical roles beyond lipid storage, and further investigation is essential to understand the importance of this unique organelle.

Chapter 2: Materials and methods

Nematode Strains

N2 Bristol, CF512 (rrf-3(b2); fem-1(hc17)), LIU1 (ldrIs[dhs-3p::dhs-3::GFP]), SJ4005 (zcIs4[hsp-4p::GFP]), SJ4100 (zcIs13[hsp-6p::GFP]), CL2070 (dvIs70[hsp-16.2p::GFP]), VS25 (hjIs[vha-6p::GFP::C34B2.10(SP12) + unc-119(+)]),EG6703 (unc-119(ed3); cxTi10816; oxEx1582[eft-3p::GFP + Cbr-unc-119]) strains were obtained from the Caenorhabditis Genetics Center (CGC). AGD1403 (uthIs387[gly-19p::xbp-1s, myo-2p::tdTomato]; zcIs4[hsp-4p::GFP]) was previously created in this lab [13]. Transgenic strains created for this study were generated from EG6703 via the MosSCI method [55] or through crossing strains.

Transgenic strains created:

AGD2192 (unc-119(ed3) III; uthSi60[vha-6p::ER-signal-sequence::mRuby::HDEL::unc-54 UTR, cb-unc-119(+)] I)

AGD2319 (unc-119(ed3) III; uthSi62[vha-6p::MLS::mRuby::unc-54 UTR, cb-unc-119(+)] I)

AGD2424 (unc-119(ed3) III; uthSi65[vha-6p::ERss::mRuby::ire-1a (344-967aa)::unc-54 3'UTR cb-unc-119(+)] IV)

AGD2425 (unc-119(ed3) III; uthSi65[vha-6p::ERss::mRuby::ire-1a (344-967aa)::unc-54 3'UTR cb-unc-119(+)] IV; zcls4[hsp-4p::GFP]V)

Worm growth and maintenance

All worms were maintained at 20°C on NGM agar plates seeded with OP50 *E. coli* bacteria. Prior to experiments, worms were bleach synchronized as described in [56], followed by overnight L1 arrest in M9 buffer (22 mM KH_2PO_4 monobasic, 42.3 mM Na_2HPO_4, 85.6 mM NaCl, 1 mM $MgSO_4$) at 20°C. For RNAi and lifespan experiments, arrested L1s were plated on 1µm IPTG, 100 µg/mL Carbenicillin NGM agar plates seeded with RNAi bacteria and maintained at 20°C.

Lifespan and tunicamycin survival assays

Lifespan analyses were conducted on NGM agar plates with specified RNAi bacteria at 20°C. Animals were moved daily for 4-7 days to new RNAi plates until progeny were no longer observed. Worms with protruding intestines, bagging phenotypes, or other forms of injury were scored as censored and not counted as part of the analysis. For combined RNAi lifespans, saturated cultures were mix 1:1 by volume. Tunicamycin survival assays were conducted with the same protocols on RNAi plates containing 25ng/uL of tunicamycin in DMSO, or equal volume of DMSO only.

Lipid droplet enrichment

CF512 worms were L1 synchronized and plated on NGM RNAi plates with Empty Vector bacteria and maintained at 25°C until day 1, after which they were moved to 20°C. ~200,000 worms were collected with M9 buffer and washed with M9 buffer + 0.1% Tween 20, followed

by 3x washes with M9 buffer. Worms were then treated with Collagenase type 3 (Worthington Biochemical, CLS-3) at 1 mg/mL in Collagenase buffer for 30 minutes at 20°C, followed by 5x washes with M9.

Lipid droplet enrichment protocols were adapted from [57]. Briefly, nematodes were washed 2x with ice-cold Buffer A and then homogenized 20x in 8 mL of Buffer A + Protease inhibitor (PI) (EMD Millipore, 20-201) using a 15 mL Dura-Grind Stainless Steel Dounce Tissue Grinder (VWR, 62400-686). Crude lysates were then transferred to 15 mL conical tubes on ice, topped to 10.5 mL with Buffer A + PI, and spun @ 1,500xG for 11 minutes at 4°C to pellet carcasses and debris. 9 mL of cleared lysates were transferred to SW41 tubes on ice and carefully layered with 3 mL of ice-cold Buffer B + PI. Samples were spun @15,000xG for 70 minutes at 4°C in an SW41 rotor without engaging breaks. The top ~1.25 mL lipid droplet "worm cream" fractions were collected into 1.5 mL tubes and frozen in liquid N_2.

Proteomic analysis of enriched lipid droplets

Proteins from frozen lipid droplet fractions were precipitated through methanol/chloroform extraction. Briefly, samples were mixed with ice-cold methanol and chloroform at 1:1:1 ratios and mixed @ 1400 RPM for 20 minutes at 4°C. Mixed samples were then spun @ 20,000xG for 10 minutes at 4°C. Upper and lower phases were collected before the precipitated proteins were washed 2x with ice-cold methanol. Proteins were briefly allowed to dry and then resuspended in 8 M urea Laemmli buffer without bromophenol blue. Protein concentrations were then quantified with a Pierce BCA Protein Assay Kit. 15-20 µg of protein were run 5-10 mm into the resolving gel of a protein gel (NuPAGE Novex, NP0336BOX) and stained with stained with Colloidal Blue (Invitrogen, LC6025). Stained protein bands were cut out and submitted to the UC Davis Proteomics Core for in-gel digest and LC-MS/MS.

RAW files were then analyzed with MaxQuant proteomics software to identify peptides based on the UniProt database *C. elegans* proteome. Briefly, trypsin was selected as the digestion enzyme, requantify (match from and to) was selected, match between run was selected, and iBAQ was selected. The remaining options were left at default settings. Contaminants, reverse, and only identified by site proteins were then removed from the list of identified proteins. The remaining proteins were then assessed for iBAQ values in all three replicates or removed. In cases of peptides matching multiple proteins, both proteins were included.

Lysate supplementation

Crude lysate was obtained from N2 worms grown on 40x concentrated EV bacteria at 20°C. ~120,000 day 1 adult worms were collected with M9 and treated with Collagenase type 3 (Worthington Biochemical, CLS-3) at 1 mg/mL in Collagenase buffer for 1 hour at 20°C. Animals were then washed 6x with M9 buffer and homogenized 20x in 3 mL of M9 buffer using a 15 mL Dura-Grind Stainless Steel Dounce Tissue Grinder (VWR, 62400-686). Crude lysate was transferred to 1.5 mL tubes and frozen in liquid N_2.

Supplementation experiments were prepared by mixing 4x concentrated RNAi bacteria with crude lysate at a 2:1 ratio, respectively. The lysate mixture was plated on RNAi plates and

allowed to dry. Dried plates were then UV irradiated without lids for 9 minutes in an ultraviolet crosslinker (UVP, CL-1000) before plating L1 arrested worms on the plate.

Fluorescent microscopy

Transcriptional reporter strains were imaged using a Leica DFC3000 G camera mounted on a Leica M205 FA microscope. Worms were grown to day 1 of adulthood at 20°C, hand-picked, and immobilized with 100 mM Sodium Azide M9 buffer on NGM agar plates. Raw images were cropped, and contrast matched using ImageJ software.

High-magnification fluorescent images were acquired with a Leica DFC9000 GT camera mounted on a Leica DM6000 B microscope. Day 1 worms were picked onto 10 mM Sodium Azide M9 buffer on slides and imaged within 15 minutes. Raw images were cropped and independently contrast optimized for clarity using ImageJ software.

Confocal images were acquired using a 3i Marianas spinning-disc confocal platform. Day 1 worms were picked onto 10 mM Sodium Azide M9 buffer on slides and imaged within 15 minutes. Raw images were cropped and independently contrast optimized for clarity using ImageJ software.

For the initial screen of *hsp-4p::GFP* animals, fluorescence was scored on the following criteria: 2 = increased fluorescence, 1 = possible increase in fluorescence, 0 = no change, -0.5 = small regions of dimmer fluorescence, -1= small regions of complete loss of fluorescence, -1.5 = globally dimmer fluorescence and some regions of no fluorescence, -2 = global loss of fluorescence and small regions of dim fluorescence, -2.5 = global loss of fluorescence except for regions within spermatheca, -3 = complete loss of fluorescence.

FRAP analysis

FRAP 4D images were acquired using a 3i Marianas spinning-disc confocal platform. Photobleaching of a 10 µm x 10 µm region within a 4 µm Z-stack was performed using a 488 nm laser for 1-2 ms. Raw images were processed with ImageJ into sum Z-projections and aligned using the “RigidBody” setting of the StackReg ImageJ plugin. FRAP analysis was performed with the FRAP Profiler ImageJ plugin by selecting the 10 µm x 10 µm photobleached region as region 1 and the total fluorescent area as region 2.

Chapter 3: *let-767*, a sterol hydrogenase, is critical for ER homeostasis

3.1 Results

A LD protein screen for modulators of the ER stress response.

The ER is a major site for both protein and lipid synthesis. Under proteotoxic stress, the ER launches genetic programs that not only result in increased chaperone expression, but also modify the ER's lipid bilayer, the site of LD biogenesis [58]. LDs function as hubs for maintaining lipid homeostasis by regulating storage and release of structural, signaling, and energy storage lipids [46]. Interestingly, they have also been shown to contribute to protein quality control [47], [54]. Here, we sought to study the functional relationship between LD quality and the ER stress response. In order to identity LD interactors, we performed a proteomic analysis of an LD enriched fraction from day 1 adult nematodes. We identified 540 LD fraction proteins, including proteins previously verified to localize to lipid droplets: DHS-3, PLIN-1, LDP-1 and ACS-4 [59]–[61]. To increase our confidence in proteins that likely interact with LDs, we performed a meta-analysis of our findings against *C. elegans* LD proteomes previously published from two independent labs [59]–[61]. We identified 120 proteins common to these three independent studies conducted with different experimental techniques **(Fig.1B).**

To determine the impact of these LD proteins on the ER stress response, we carried out an RNAi screen to identity genes which altered induction of the UPR^{ER} under conditions of proteotoxic stress. We utilized a transcriptional reporter composed of the *hsp-4* (*C. elegans* Hsp70/BiP chaperone protein) promoter driving GFP expression (*hsp-4p::GFP*) to assess the UPR^{ER} induction and *sec-11* (an ER serine-peptidase) RNAi to generate ER stress and robustly induce the GFP reporter **(Fig.1C)**. In combination with the *sec-11* RNAi, we individually knocked down our 120 candidate LD genes to perform a double RNAi screen. Of the available RNAis for the 120 candidates, we found that interference of 49 genes led to reduced induction of the UPR^{ER} reporter **(Table 1)**. While a large portion of these genes are annotated as functioning in general transcription or translation (*e.g*. ribosomal subunits), a subset of 11 were potential novel modulators of the UPR^{ER} **(Fig.1C)**.

LET-767, a hydroxysteroid dehydrogenase, is critical for ER homeostasis.

Our initial literature search of the 11 genes highlighted *let-767* as the only gene previously characterized to directly affect lipid metabolism. LET-767 is a hydroxysteroid dehydrogenase implicated in monomethyl branched-chain fatty acids (mmBCFA) synthesis and steroid metabolism, as well as being necessary for normal growth and reproductive development [62]–[64]. Since *let-767* has been shown to be primarily expressed in the intestine and localize to the ER [62], we determined the impact of *let-767* RNAi on intestinal LDs and ER. We found that knockdown of *let-767* caused a significant reduction in LD size and number, as well as significant disruption of the ER morphology. To determine whether these perturbations were restricted to LDs and the ER or a more global phenotype, we also examined the effect of *let-767* RNAi on mitochondrial morphology. The RNAi treatment resulted in a severely fragmented network and enlarged mitochondria **(Fig2.A)**.

Due to the severe defects in organelle morphology, we tested whether *let-767* RNAi alone would induce the UPR^{ER} or the UPR^{mito}. Surprisingly, these animals only displayed a mild induction of the UPR^{ER} and no activation of the UPR^{mito}. However, under conditions of stress, only the UPR^{ER} induction was compromised **(Fig.2B-C)**. To further test whether the stress response suppression was specific to the ER or due to general defects in these animals, we tested the heat shock response (HSR). *let-767* RNAi had no effect on basal or heat-stress induced activation of the HSR **(Fig.2D)**, indicating that *let-767* plays a specific role in maintaining ER homeostasis.

let-767 mediated UPR^{ER} suppression is not due to loss of mmBCFAs

In agreement with previous studies, we observed a gross reduction in animal size and reproductive capacity with *let-767* RNAi treatment **(Fig.3A)**. Previous work has implicated *let-*767 as the 3-keto acyl reductase in mmBCFA synthesis required for normal F1development, primarily C17 mmBCFA (isoC17) synthesis [62], [65]. While phenotypes associated with loss of *let-767* have been shown to be amplified by cholesterol depletion [64], these enhancements were likely due to the role of isoC17 in cholesterol mobilization [66]. To determine whether the defects we observed in *let-767* knockdown animals were a result of insufficient mmBCFAs, we supplemented animals grown on *let-767* RNAi with exogenous isoC17. Supplementation of the C17 mmBCFA did not rescue *let-767* RNAi treated animal growth or reproductive development. However, isoC17 supplementation was able to rescue the F1 larval arrest of RNAi targeting *elo-5*, the elongase mainly responsible for isoC17 production [67], suggesting that isoC17 mmBCFA was properly delivered to the animals **(Fig.3A)**. Similarly, isoC17 supplementation was not able to rescue the suppressed UPR^{ER} signaling or disrupted ER morphology caused by *let-767* knockdown **(Fig.3B-C)**, suggesting that the ER phenotypes are not simply due to insufficient mmBCFA synthesis.

Due to the ineffective rescue of mmBCFA supplementation and the general depletion lipid droplets, we questioned whether a complete panel of lipids would be able to rescue the phenotypes. To this end, we supplemented animals grown on *let-767* RNAi with crude lysate isolated from wild type (N2) animals, which would likely contain all the essential lipids for *C. elegans* survival and development. Indeed, supplementing crude lysate improved the ER morphology to near wild-type conditions, as well as the abundance and size of lipid droplets **(Fig.3D)**. Surprisingly, the restored ER morphology and improved growth did not reestablish normal UPR^{ER} signaling in response to ER stress **(Fig.3E)**, implying distinct functional mechanisms for *let-767* dependent changes on ER morphology and UPR^{ER} activation.

Knockdown of the *let-767* metabolic pathway restores signaling of the UPR^{ER}

Since the supplementation of all essential lipids was not sufficient to recover the UPR^{ER} signaling to WT levels, we considered the possibility that UPR^{ER} signaling could be compromised in *let-767* knockdown animals due to the accumulation of a toxic metabolic intermediate. To test this hypothesis, we coupled *let-767* RNAi with knockdown of *sbp-1*, the ortholog of human SREBP, a major transcriptional regulator of key enzymes within the isoC17 metabolic pathway [68]. Indeed, analysis of a previously published RNAseq dataset of *sbp-1*

RNAi treated nematodes confirmed downregulation of mmBCFA associated genes including *let-767* and *elo-5* [69]. From our double RNAi of *sbp-1* and tandem *let-767/sec-11*, we observed a significant recovery of stress-induced UPR^{ER} signaling in *let-767* knockdown animals **(Fig.4A)** and a marked improvement in animal size and reproductive development. Moreover, *sbp-1* RNAi greatly improved the lifespan defects of *let-767* knockdown animals **(Fig.4B)**. Similarly, *sbp-1* knockdown rescued the survival of *let-767* RNAi treated animals under the proteotoxic ER stress of Tunicamycin, an N-linked glycosylation inhibitor **(Fig.4C-D)**. Lastly, we determined whether *sbp-1* RNAi could also suppress the defects in ER morphology caused by *let-767* knockdown. As expected, we observed a depletion of lipid droplets and a slight perturbation of the ER morphology with *sbp-1* RNAi **(Fig.4D)**. More importantly, under *let-767* RNAi conditions, *sbp-1* RNAi had only mild effects on ER and lipid droplet morphology, suggesting that limiting the *let-767* metabolic pathway through *sbp-1* knockdown is not enough to restore ER and LD morphology. However, in the presence of crude lysate, both *sbp-1* RNAi alone or combined with *let-767* RNAi resulted in ER and lipid droplet morphology resembling WT animals **(Fig.4D)**. These results are congruent with SREBP's central role in maintaining lipid homeostasis [24]. While reducing the *let-767* metabolic pathway restores UPR^{ER} signaling, loss of additional lipid pathways requires that those lipids be supplemented to maintain lipid homeostasis. Moreover, these data indicate that LET-767 function impacts two aspects of ER quality: lipid synthesis required for proper organelle morphology and turnover of a toxic metabolite which negatively impacts the ER stress response.

Compromised UPR^{ER} through reduced membrane quality in *let-767* knockdown animals.

Finally, we sought to determine how potential accumulation of a metabolite in *let-767* knockdown animals could impact the UPR^{ER}. The isoC17 pathway has been previously hypothesized to produce a toxic metabolite that can alter membrane quality and signaling [70]. Therefore, we considered the possibility that accumulation of a metabolite from the *let-767* pathway could be altering the ER membrane and preventing UPR^{ER} signaling, resulting in decreased organelle function and overall health. To determine if the membrane quality was perturbed, we probed ER membrane dynamics by performing Fluorescence Recovery After Photobleaching (FRAP) utilizing luminal and transmembrane ER fluorescent markers [71]. From our analysis, we observed that *let-767* knockdown resulted in a highly reduced mobile fractions of both luminal and membrane markers, consistent with animals exhibiting general defects in ER morphology and membrane dynamics. Upon lysate supplementation, the luminal mobile fraction of *let-767* knockdown animals had a significant recovery to 80% of WT level, while the membrane marker mobile fraction only recovered to 54% of WT suggested that the membrane mobility is much more disrupted by *let-767* RNAi **(Fig.5A-B)**.

Proper UPR^{ER} signaling is dependent on dimerization of IRE-1 to splice *xbp-1* mRNA to its active *xbp-1s* form [5]. Therefore, one possibility is that decreased membrane mobility impedes IRE-1 activity, leading to a compromised ER stress response. To test this hypothesis, we examined the impact of *let-767* knockdown on ectopic UPR^{ER} activation at two different points along the same mechanistic pathway: 1) overexpression of *ire-1*, which would require proper IRE-1 dimerization, and 2) overexpression of the active *xbp-1s* isoform, which would

bypass the requirement of IRE-1 dimerization. While over-expression of full-length *ire-1* (*ire-1a OE*) proved to be lethal, over-expression of *ire-1* lacking a significant portion of the luminal domain (*ire-1b OE*) was viable. By creating an RNAi targeting the luminal domain, we confirmed that intestinal *ire-1b* OE was sufficient to induce intestinal UPR^{ER} signaling without the endogenous *ire-1a* **(Fig.5C-D)**. As expected, *let-767* knockdown resulted in a considerable reduction of *ire-1b OE* mediated UPR^{ER} induction. More importantly, *let-767* knockdown only mildly reduced *xbp-1s OE* induction of the UPR^{ER}, suggesting that *xbp-1s* can at least partly bypass the detrimental effects of *let-767* RNAi on the ER stress response **(Fig.5E-F)**. These data strongly support our hypothesis that *let-767* knockdown compromises induction of the UPR^{ER} by interfering with IRE-1 activity and subsequent splicing of *xbp-1* mRNA.

3.2 Discussion

Cells must be able to monitor and maintain both lipid and protein homeostasis to preserve cellular function. The ER is uniquely a major site of lipid synthesis and protein trafficking, supplying lipids to multiple organelles and processing a third of the cell's proteins. The ER is also responsible for the biogenesis of lipid droplets, the cell's lipid storage organelle. Along with their lipid regulating functions, lipid droplets have also been shown to contribute to protein quality control. Here, we aimed to assess the functional relationship between lipid droplets and the ER's protein quality control system, the UPR^{ER}. In doing so, we identified the ER protein, LET-767, as a novel regulator of ER homeostasis.

Through our screen of lipid droplet associated proteins, we found that LET-767 function was necessary for proper induction of the UPR^{ER}. Interestingly, LET-767 localizes to the ER and not lipid droplets, as detected by fluorescence microscopy [62]. Consistent with this localization, LET-767 is predicted to contain an ER signal sequence and at least one transmembrane domain (http://topcons.cbr.su.se/). Our list of candidate lipid droplet proteins containing LET-767 was derived from LD proteomes isolated by two independent labs [59]–[61]. While this comparison improves our confidence in potential lipid droplet interacting proteins, it does not verify their interaction. Lipid droplets are generally isolated through their buoyancy due to their high lipid content [57]. As a result of their direct interaction with multiple organelles, LD isolations naturally contain associated membranes and their proteins [72]. Nonetheless, it is worth noting that the closest mammalian orthologs of *let-767* (HSD17B3, HSD17B12, and HSDL1) have also been identified in mammalian LD isolations [73], [74]. While not likely to be directly localized to lipids droplets, our evidence shows that LET-767 function has a definite impact on lipid droplet and ER morphology, though whether LET-767 plays direct role in lipid droplet biogenesis on the ER membrane remains to be established.

let-767 has been previously characterized as a 3-ketoacyl-CoA reductase involved in isoC17 fatty acid elongation and as a 17β-hydroxysteroid dehydrogenase capable of metabolizing steroid hormones in mammalian cells [62], [63]. mmBCFAs have been shown to be required for development in *C. elegans*, likely through synthesis of d17iso-glucosylceramide, a glycosphingolipid involved in cholesterol mobilization and TORC1 signaling [66], [75]. In this study, isoC17 supplementation did not rescue growth, organelle morphology, or UPR^{ER} phenotypes. Yet, consistent with a reduction in isoC17 synthesis, we did observe an increased requirement for cholesterol in *let-767* knockdown animals grown in dense conditions (data now shown). Growth and morphology phenotypes of *let-767* knockdown were however, rescued by complete lipid supplementation by means of crude lysate. Multiple steroid hormones have been identified in *C. elegans* and could be potential metabolites of LET-767, which eventually alter lipid pathways through binding of nuclear hormone receptors [76]. Supplementation of these potential ligands through crude lysate would then be expected to rescue *let-767* knockdown phenotypes, although, to date, *let-767* has not been implicated in any specific sterol pathway in *C. elegans*. Interestingly, the complete lipid supplementation was unable to restore UPR^{ER} signaling and indicated to us that in addition to the loss of LET-767 products, accumulation of its substrates could also be contributing to the *let-767* knockdown phenotypes. This evidence and

the compromised ER, mitochondrial, and lipid droplet organelles of *let-767* knockdown suggest a more complex role for LET-767 in lipid metabolism than is currently known.

Sensors within the ER membrane are capable of detecting membrane lipid disequilibrium and activating the UPR^{ER} [26], [27]. Here we find a contrasting response: knockdown of the lipid enzyme, *let-767*, results in suppression of the UPR^{ER}. We hypothesized that accumulation of a toxic LET-767 substrate could be disrupting the ER membrane and compromising membrane function. As dimerization of IRE-1 is required for its signaling function [5], reduced membrane mobility could certainly impact IRE-1 interactions, thereby suppressing the UPR^{ER} by preventing IRE-1 mediated splicing of *xbp-1* to *xbp-1s*. Indeed, by knocking down *sbp-1*, a transcription factor upstream of the *let-767* lipid pathway [68], [69], we observed a significant rescue of the UPR^{ER}, as well as improved lifespan and ER stress survival. Thus, it is likely that LET-767 processes a lipid metabolite downstream of *sbp-1* that is essential to maintaining membrane dynamics and ultimately, induction of the UPR^{ER}.

Interestingly, while *sbp-1* knockdown ameliorated the defects in UPR^{ER} induction, growth, and organismal health in *let-767* knockdown animals, there was no effect on organelle morphology. Although knockdown of *sbp-1* potentially prevents the accumulation of the LET-767 substrate to alleviate detrimental phenotypes, as a transcription factor for major lipogenic pathways [24], *sbp-1* knockdown likely failed to fully rescue organelle morphology of *let-767* deficient animals due to insufficient lipid production. Thus, *let-767* knockdown animals require lipid supplementation for full restoration of organelle morphology, hinting that some of the phenotypes are a result of insufficient lipid production. While this reduction in lipids may be due to changes in nuclear hormone ligand production, as previously mentioned, a compromised ER membrane could instead be the cause due to the major role the ER membrane plays in lipid production.

Through FRAP microscopy we then determined whether ER dynamics were in fact disrupted by *let-767* knockdown. We found that both membrane and luminal mobility was significantly impacted by *let-767* RNAi. While changes in global lipid metabolism and ER structure are a potential cause of altered luminal dynamics, we observed that by restoring ER morphology through supplementation of essential lipids via crude lysate, only the membrane mobile fraction remained substantially reduced. These data provide additional evidence that a potential LET-767 toxic substrate is altering ER membrane quality independent of its effects on lipid production.

UPR^{ER} induction through ectopic expression of *xbp-1s* would be independent of ER membrane functionality, as this would bypass the need of IRE-1 oligomerization and subsequent splicing of *xbp-1* mRNA. We find that in *let-767* knockdown animals, induction of UPR^{ER} via *ire-1b* overexpression was significantly reduced, while UPR^{ER} induction via *xbp-1s* overexpression was only mildly affected. Although the generally reduced health of *let-767* knockdown animals may impact UPR^{ER} induction, our evidence supports a model where LET-767 impacts UPR^{ER} induction via ER membrane homeostasis and IRE-1 function.

In our current model, *let-767* is required to maintain ER homeostasis. While we are currently investigating which specific lipids are regulated by LET-767, its function clearly affects both lipid and protein homeostasis. Loss of *let-767* results in accumulation of substrate metabolites, which disrupt transmembrane protein function, thereby reducing UPR^{ER} signaling and lipid synthesis. While exogenous lipids can compensate for deficient lipid synthesis, restoration of UPR^{ER} signaling requires knockdown of the *let-767* pathway to eliminate disruptive metabolite accumulation at the membrane **(Fig.6)**.

3.3 Figures

Table 1. Candidate LD proteins identified by proteomics meta-analysis

Gene Name	Sequence Name	Gene Description	Screen Score	Screen Stage
inf-1	F57B9.6	Eukaryotic initiation factor 4A	-3	L4/Adult
rpl-10	F10B5.1	60S ribosomal protein L10	-3	L4/Adult
rpl-13	C32E8.2	60S ribosomal protein L13	-3	L3/L4
rpl-16	M01F1.2	60S ribosomal protein L13a	-3	L2/L3
rpl-17	Y48G8AL.8	60S ribosomal protein L17	-3	L4/Adult
rpl-19	C09D4.5	60S ribosomal protein L19	-3	L3
rpl-20	E04A4.8	60S ribosomal protein L18a	-3	Adult
rpl-23	B0336.10	60S ribosomal protein L23	-3	Adult
rpl-3	F13B10.2	60S ribosomal protein L3	-3	L3
rpl-35	ZK652.4	60S ribosomal protein L35	-3	L3/L4
rpl-9	R13A5.8	60S ribosomal protein L9	-3	L4/Adult
rps-0	B0393.1	40S ribosomal protein SA	-3	Adult
rps-1	F56F3.5	40S ribosomal protein S3a	-3	L3
rps-10	D1007.6	Ribosomal Protein, Small subunit	-3	Adult
rps-16	T01C3.6	40S ribosomal protein S16	-3	Adult
rps-18	Y57G11C.16	Ribosomal Protein, Small subunit	-3	L3/L4
rps-19	T05F1.3	40S ribosomal protein S19	-3	Adult
rps-20	Y105E8A.16	Ribosomal Protein, Small subunit	-3	L4/Adult
rps-3	C23G10.3	40S ribosomal protein S3	-3	L3/L4
rps-5	T05E11.1	40S ribosomal protein S5	-3	Adult
rps-8	F42C5.8	40S ribosomal protein S8	-3	L4/Adult
rps-9	F40F8.10	40S ribosomal protein S9	-3	L3/L4
atp-1	H28O16.1	ATP synthase subunit alpha, mitochondrial	-2.5	L3/L4
eef-1A.1	F31E3.5	Elongation factor 1-alpha	-2.5	Adult
eef-2	F25H5.4	Elongation factor 2	-2.5	Adult
rla-0	F25H2.10	60S acidic ribosomal protein P0	-2.5	Adult
rpl-2	B0250.1	60S ribosomal protein L8	-2.5	L4/Adult
rpl-22	C27A2.2	60S ribosomal protein L22	-2.5	L4/Adult
rpl-27	C53H9.1	60S ribosomal protein L27	-2.5	Adult
rpl-36	F37C12.4	60S ribosomal protein L36	-2.5	L4/Adult
rpl-6	R151.3	60S ribosomal protein L6	-2.5	Adult
rps-14	F37C12.9	40S ribosomal protein S14	-2.5	Adult
rps-15	F36A2.6	40S ribosomal protein S15	-2.5	Adult
rps-22	F53A3.3	Ribosomal Protein, Small subunit	-2.5	L4/Adult
rps-7	ZC434.2	40S ribosomal protein S7	-2.5	Adult

atp-2	C34E10.6	ATP synthase subunit beta, mitochondrial	-2	L3/L4
fib-1	T01C3.7	rRNA 2'-O-methyltransferase fibrillarin	-2	Adult
rab-1	C39F7.4	RAB family	-2	L3/L4
rpl-18	Y45F10D.12	60S ribosomal protein L18	-2	Adult
rpl-5	F54C9.5	60S ribosomal protein L5	-2	Adult
rps-11	F40F11.1	Ribosomal Protein, Small subunit	-2	Adult
rps-2	C49H3.11	40S ribosomal protein S2	-2	Adult
hsp-1	F26D10.3	Heat shock 70 kDa protein A	-1.5	Adult
hsp-90	C47E8.5	Heat shock protein 90	-1.5	Adult
let-767	C56G2.6	Very-long-chain 3-oxooacyl-coA reductase let-767	-1.5	Adult
tba-2	C47B2.3	Tubulin alpha-2 chain	-1.5	Adult
ucr-1	F56D2.1	Cytochrome b-c1 complex subunit 1, mitochondrial	-1.5	Adult
vha-13	Y49A3A.2	V-type proton ATPase catalytic subunit A	-1.5	L3/L4
vha-15	T14F9.1	Probable V-type proton ATPase subunit H 2	-1.5	L3/L4
act-4	M03F4.2	Actin-4	-1	Adult
ant-1.1	T27E9.1	Adenine Nucleotide Translocator	-1	Adult
atad-3	F54B3.3	ATPase family AAA domain-containing protein 3	-1	Adult
eat-6	B0365.3	Sodium/potassium-transporting ATPase subunit alpha	-1	Adult
eef-1G	F17C11.9	Probable elongation factor 1-gamma	-1	L4/Adult
F42G8.10	F42G8.10	NADH:ubiquinone oxidoreductase subunit B11	-1	Adult
hsp-60	Y22D7AL.5	Chaperonin homolog Hsp-60, mitochondrial	-1	Adult
T02H6.11	T02H6.11	ubiquinol-cytochrome c reductase binding protein	-1	Adult
tba-4	F44F4.11	Tubulin alpha chain	-1	Adult
Y7A5A.1	Y7A5A.1	24-dehydrocholesterol reductase	-1	Adult
acs-17	C46F4.2	Fatty Acid CoA Synthetase family	-0.5	Adult
ant-1.3	K01H12.2	Adenine Nucleotide Translocator; Mitochondrial	-0.5	Adult
B0491.5	B0491.5	enriched in the OLL, the PVD, and the germ line	-0.5	Adult
gdh-1	ZK829.4	Glutamate dehydrogenase	-0.5	Adult
ldp-1	F22F7.1	Lipid droplet localized protein	-0.5	Adult
nuo-2	T10E9.7	NADH Ubiquinone Oxidoreductase	-0.5	Adult
rab-7	W03C9.3	RAB family	-0.5	Adult
rack-1	K04D7.1	Guanine nucleotide-binding protein subunit beta-2-like 1	-0.5	Adult
rpl-31	W09C5.6	60S ribosomal protein L31	-0.5	Adult
rps-4	Y43B11AR.4	40S ribosomal protein S4	-0.5	Adult
algn-2	F09E5.2	Asparagine Linked Glycosylation (ALG) homolog, Nematode	0	Adult
alh-8	F13D12.4	Probable methylmalonate-semialdehyde dehydrogenase	0	Adult
cgh-1	C07H6.5	ATP-dependent RNA helicase cgh-1	0	Adult
cts-1	T20G5.2	Probable citrate synthase, mitochondrial	0	Adult
D2030.4	D2030.4	NADH dehydrogenase	0	Adult
dhs-19	T11F9.11	DeHydrogenases, Short chain	0	Adult
dhs-3	T02E1.5	DeHydrogenases, Short chain	0	Adult

F01G4.6	F01G4.6	Phosphate carrier protein, mitochondrial	0	Adult
F44B9.5	F44B9.5	Ancient ubiquitous protein 1 homolog	0	Adult
F52H2.6	F52H2.6	Diminuto-like protein	0	Adult
lec-1	W09H1.6	32 kDa beta-galactoside-binding lectin	0	Adult
par-5	M117.2	14-3-3-like protein 1	0	Adult
pdi-2	C07A12.4	Protein disulfide-isomerase 2	0	Adult
phb-2	T24H7.1	Mitochondrial prohibitin complex protein 2	0	Adult
plin-1	W01A8.1	Perilipin-1 homolog	0	Adult
rpl-32	T24B8.1	Ribosomal Protein, Large subunit	0	Adult
tba-7	T28D6.2	Tubulin alpha chain	0	Adult
tomm-20	F23H12.2	Mitochondrial import receptor subunit TOM20 homolog	0	Adult
unc-108	F53F10.4	RAB2A, member RAS oncogene family	0	Adult
vdac-1	R05G6.7	Probable voltage-dependent anion-selective channel	0	Adult
vit-1	K09F5.2	Vitellogenin-1	0	Adult
vit-2	C42D8.2	Vitellogenin-2	0	Adult
vit-6	K07H8.6	Vitellogenin-6	0	Adult
acs-4	F37C12.7	Fatty Acid CoA Synthetase family	0.5	Adult
tbb-1	K01G5.7	Tubulin beta chain	0.5	Adult
alh-4	T05H4.13	Aldehyde dehydrogenase	1	Adult
enpl-1	T05E11.3	Endoplasmin homolog	1	Adult
hsp-3	C15H9.6	Heat shock 70 kDa protein C	1	Adult
vit-5	C04F6.1	Vitellogenin-5	1	Adult
hsp-4	F43E2.8	Endoplasmic reticulum chaperone BiP homolog	2	Adult
ben-1	C54C6.2	Tubulin beta chain	N/A	N/A
dhs-9	Y32H12A.3	DeHydrogenases, Short chain	N/A	N/A
eef-1A.2	R03G5.1	Elongation factor 1-alpha	N/A	N/A
faah-4	Y56A3A.12	Fatty Acid Amide Hydrolase homolog	N/A	N/A
rpl-1	Y71F9AL.13	60S ribosomal protein L10a	N/A	N/A
rpl-15	K11H12.2	60S ribosomal protein L15	N/A	N/A
rpl-21	C14B9.7	60S ribosomal protein L21	N/A	N/A
rpl-4	B0041.4	60S ribosomal protein L4	N/A	N/A
rpl-7	F53G12.10	60S ribosomal protein L7	N/A	N/A
rpl-7A	Y24D9A.4	60S ribosomal protein L7a	N/A	N/A
rps-13	C16A3.9	40S ribosomal protein S13	N/A	N/A
rps-28	Y41D4B.5	40S ribosomal protein S28	N/A	N/A
rps-6	Y71A12B.1	40S ribosomal protein S6	N/A	N/A
sip-1	F43D9.4	Stress-induced protein 1	N/A	N/A
trap-1	Y71F9AM.6	TRanslocon-Associated Protein	N/A	N/A
tsn-1	F10G7.2	Staphylococcal nuclease domain-containing protein	N/A	N/A
vha-11	Y38F2AL.3	V-type proton ATPase subunit C	N/A	N/A
vit-4	F59D8.2	Vitellogenin-4	N/A	N/A

Y53F4B.18	Y53F4B.18	fatty acid amide hydrolase 2	N/A	N/A
Y69A2AR.18	Y69A2AR.18	ATP synthase F1 subunit gamma	N/A	N/A
ZK809.3	ZK809.3	X-ray repair cross complementing 5	N/A	N/A

Table 1. Candidate LD proteins identified by proteomics meta-analysis

Proteins identified in meta-analysis of LD isolation proteomics. Gene description, screen score, and developmental stage at time of screen noted. N/A corresponds to genes not screened due to RNAi availability.

Figure 1. Identification of LD-associated proteins involved in ER quality control

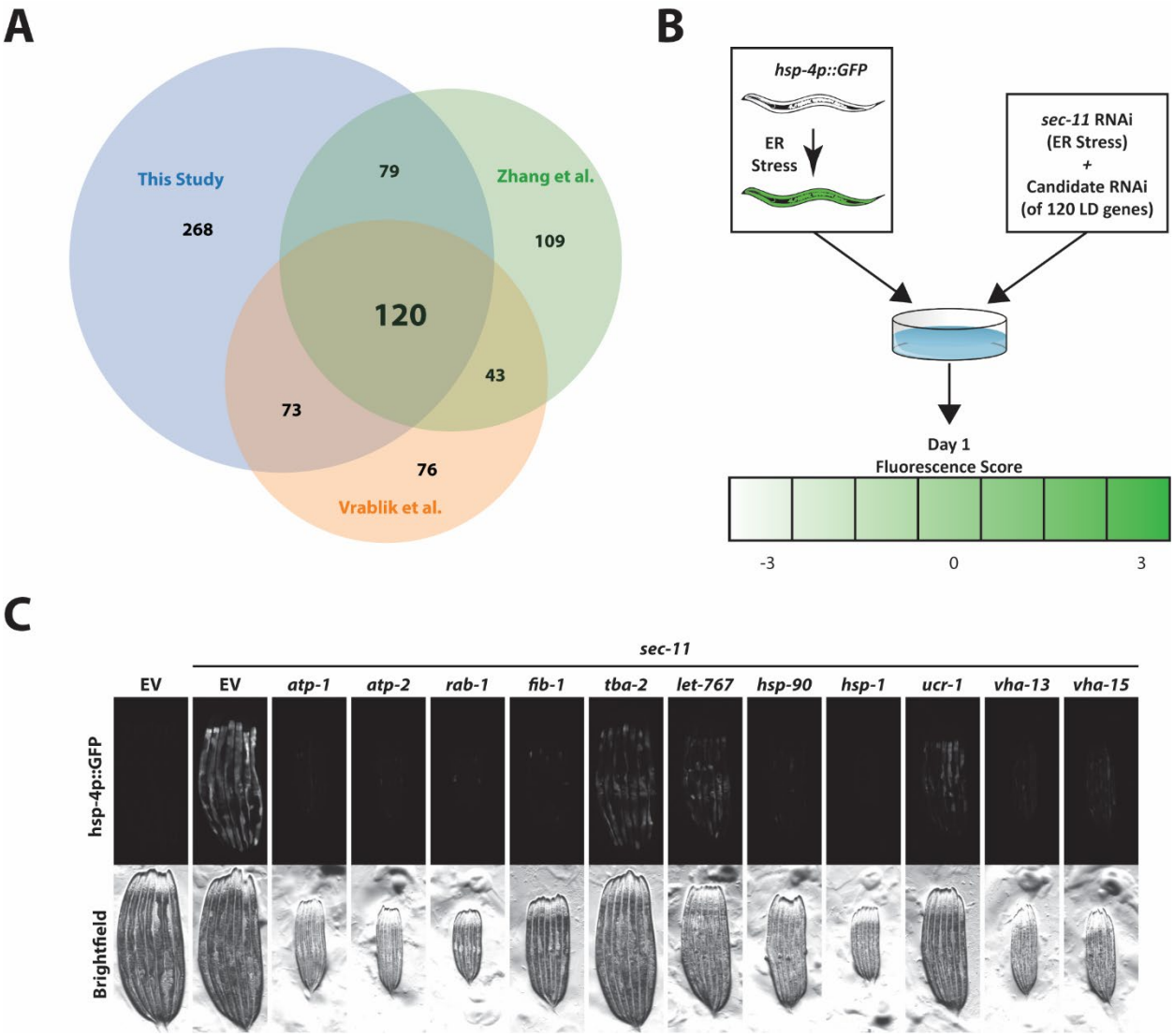

Figure 1. Identification of LD-associated proteins involved in ER quality control

(A) Venn-diagram summarizing meta-analysis of this study's LD isolation proteomics against previously published *C. elegans* LD isolation proteomes. (B) Schematic for screening method used to identify UPR^{ER} modulators from candidate LD-associated proteins. (C) Transgenic animals expressing *hsp-4p::GFP* grown on Empty Vector or *sec-11* RNAi combined with either *atp-1, atp-2, rab-1, fib-1, tba-2, let-767, hsp-90, hsp-1, ucr-1, vha-13*, or *vha-15* RNAi to assess effects on UPR^{ER} induction. All images contrast matched.

Figure 2. *let-767* as a novel regulator of ER quality control

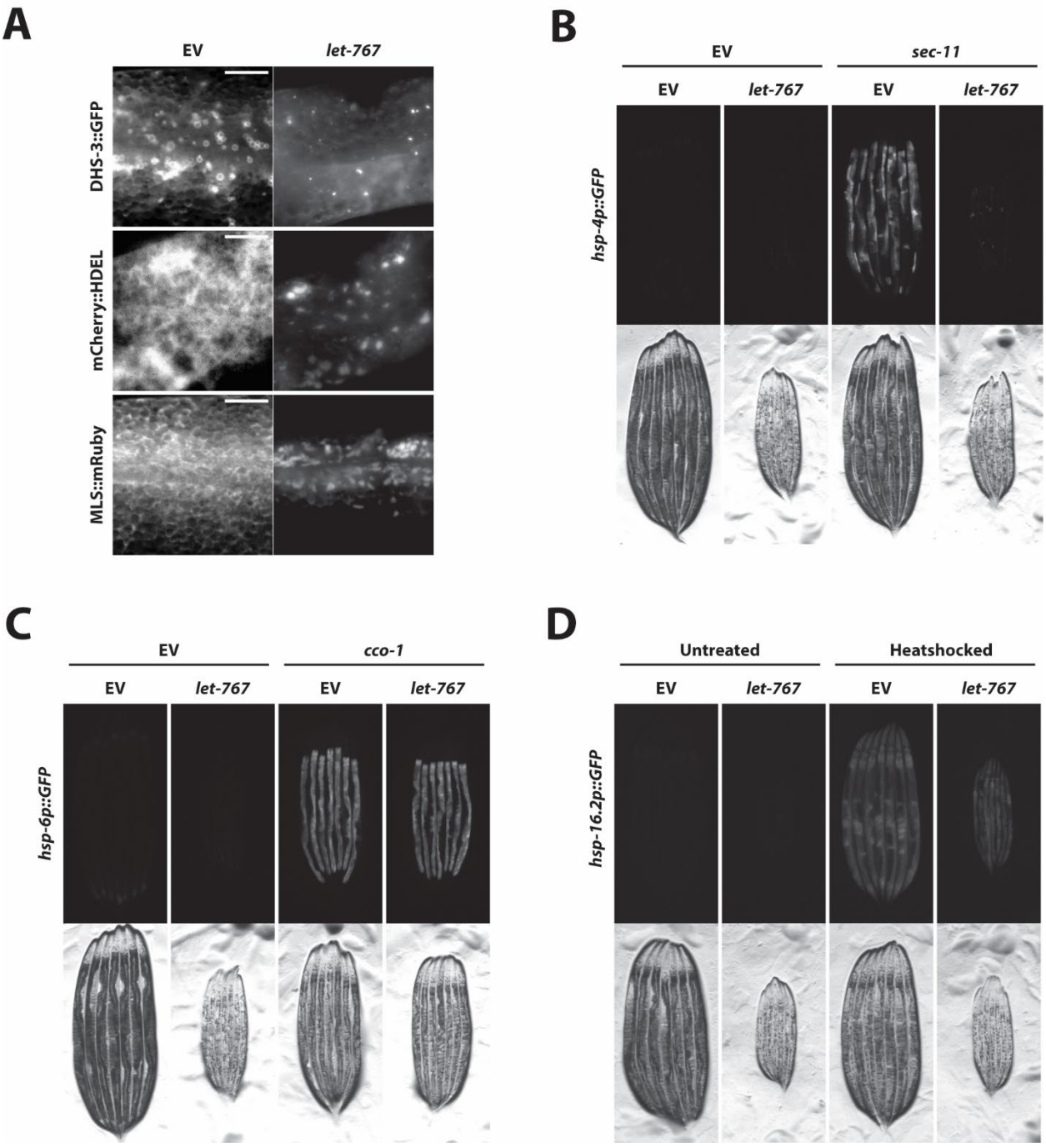

Figure 2. *let-767* as a novel regulator of ER quality control

(A) Transgenic animals expressing intestinal *dhs-3::GFP*, *mCherry::HDEL*, or *mls::mRuby* grown on Empty Vector or *let-767* RNAi to characterize lipid droplet, ER, and mitochondrial morphology, respectively. Scale bar: 10 µm. (B) Transgenic animals expressing *hsp-4p::GFP*, grown on Empty Vector, *let-767*, and/or *sec-11* RNAi to asses UPR^{ER} induction. Empty Vector used as control or *sec-11* RNAi for induction of ER stress. (C) Transgenic animals expressing *hsp-6p::GFP*, grown on Empty Vector, *let-767*, and/or *cco-1* RNAi to asses UPR^{mito} induction. Empty Vector used as control or *cco-1* RNAi for induction of mitochondrial stress. (D) Transgenic animals expressing *hsp-16.2p::GFP* grown on Empty Vector or *let-767* RNAi with or without heat-shock treatment to asses heat shock response. Animals imaged 2 hours after recovery at 20C°. Images for all transcriptional reporters contrast matched. Images in (A) contrast enhanced individually for clarity.

Figure 3. Whole animal lysate rescues defects in ER morphology but not UPR^{ER} induction

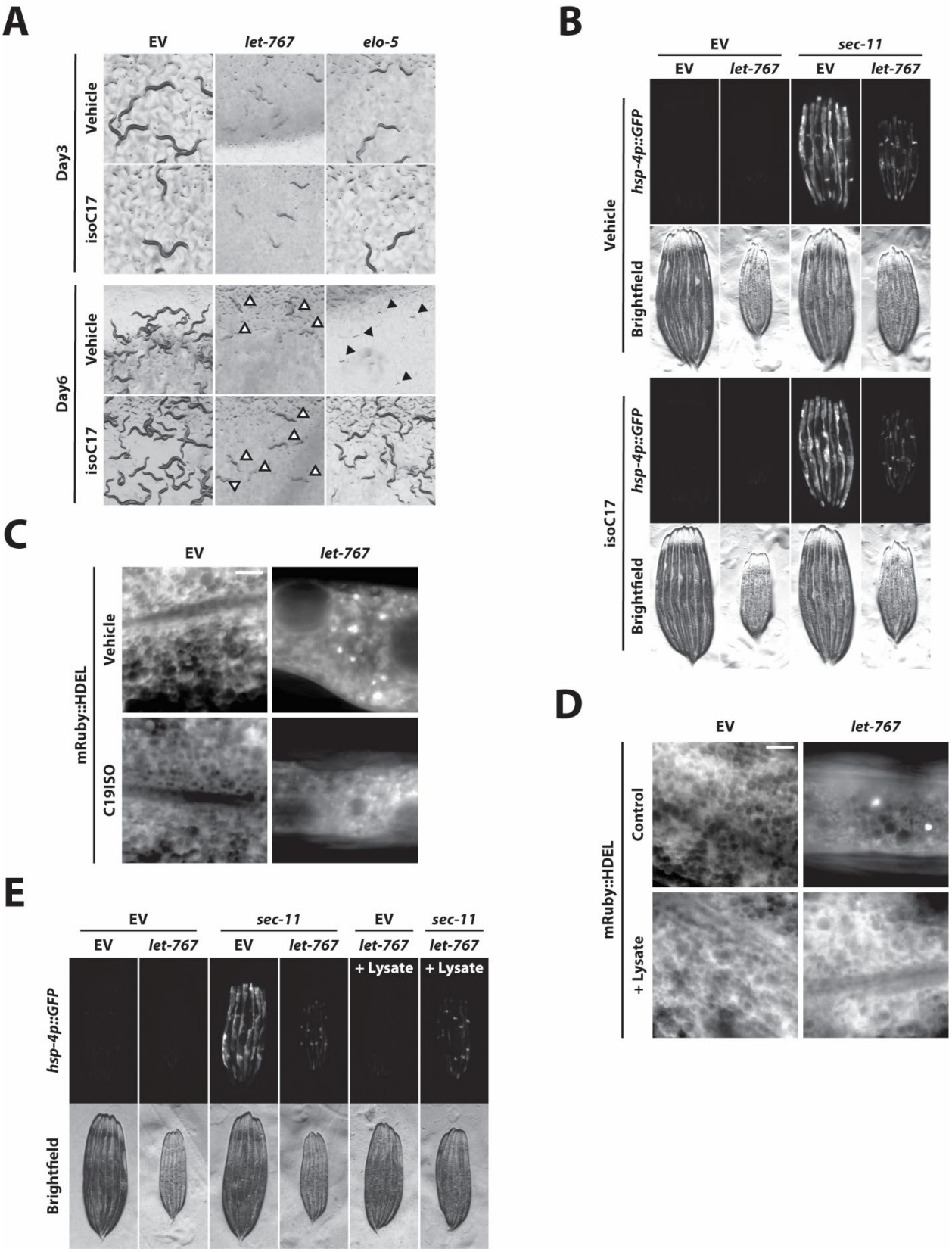

Figure 3. Whole animal lysate rescues defects in ER morphology but not UPR^{ER} induction

(A) P_0 N2 animals 3 days after synchronization or F_1 progeny 6 days after initial synchronization on Empty Vector, *let-767*, or *elo-5* RNAi bacteria grown in vehicle or isoC17 mmBCFA supplemented media to assess supplementation efficacy. Black arrows denote F_1 animals arrested at L1 stage. White arrows denote P_0 animals at day 6. (B) Transgenic animals expressing *hsp-4p::GFP* grown on Empty Vector or *let-767* RNAi combined with Empty Vector or *sec-11* RNAi to asses UPR^{ER} induction. Bacteria grown in media supplemented with vehicle or isoC17 mmBCFA. (C) Transgenic animals expressing an intestinal *mRuby::HDEL* ER marker grown on Empty Vector or *let-767* RNAi bacteria grown in vehicle or isoC17 mmBCFA supplemented media to asses ER morphology. Scale bar: 5 μm. (D) Transgenic animals expressing intestinal *mRuby::HDEL* grown on Empty Vector or *let-767* RNAi mixed at 2:1 ratio with vehicle or lysate to asses ER morphology. Scale bar: 5 μm. (E) Transgenic animals expressing *hsp-4p::GFP* grown on Empty Vector or *let-767* RNAi combined with Empty Vector or *sec-11* RNAi mixed with lysate to assess UPR^{ER} induction. RNAi mixed 1:1:1 ratio with vehicle or crude lysate. Images for transcriptional reporters contrast matched. Images for (C) and (D) contrasted enhanced individually for clarity.

Figure 4. Reduced lipid synthesis ameliorates *let-767* knockdown defects in the UPR^{ER} induction

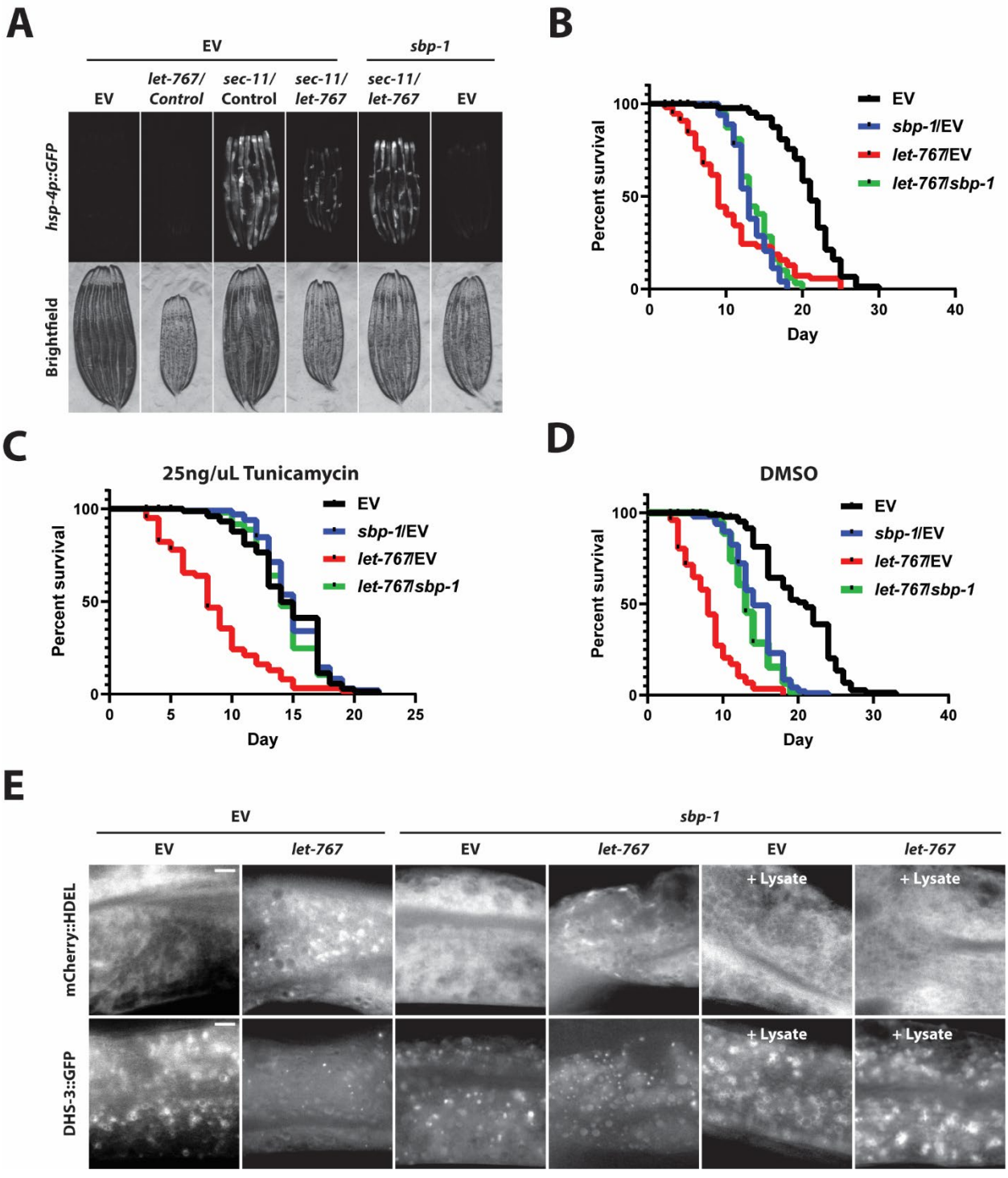

Figure 4. Reduced lipid synthesis ameliorates *let-767* knockdown defects in the UPR^{ER} induction

(A) Transgenic animals expressing *hsp-4p::GFP* grown on Empty Vector or *let-767/Control*, *sec-11/Control*, *sec-11/let-767* tandem RNAis mixed with Empty Vector or *sbp-1* RNAi to asses UPR^{ER} induction. *tdTomato* sequence used as *Control*. Images contrast matched. (B) Lifespans of N2 animals grown on Empty Vector or *let-767* RNAi combined with Empty Vector or *sbp-1* RNAi. (C-D) Concurrent survival assays of N2 animals transferred to ER stress conditions of 25 ng/uL Tunicamycin (C) or control DMSO (D) conditions at day 1 of adulthood. Animals continuously grown on Empty Vector or *let-767* RNAi combined with Empty Vector or *sbp-1* RNAi from L1 synchronization. (E) Transgenic animals expressing intestinal *mCherry::HDEL* or *dhs-3::GFP* grown on Empty Vector or *let-767* RNAi combined with Empty Vector or *sbp-1* RNAi to asses ER and LD morphology. RNAi mixed with vehicle or lysate at 1:1:1: ratio. ER and LD images acquired and contrast enhanced individually to maximize organelle image quality. Scale bar: 5 μm.

Figure 5. *let-767* mediated suppression of the UPR^{ER} through altered membrane dynamics

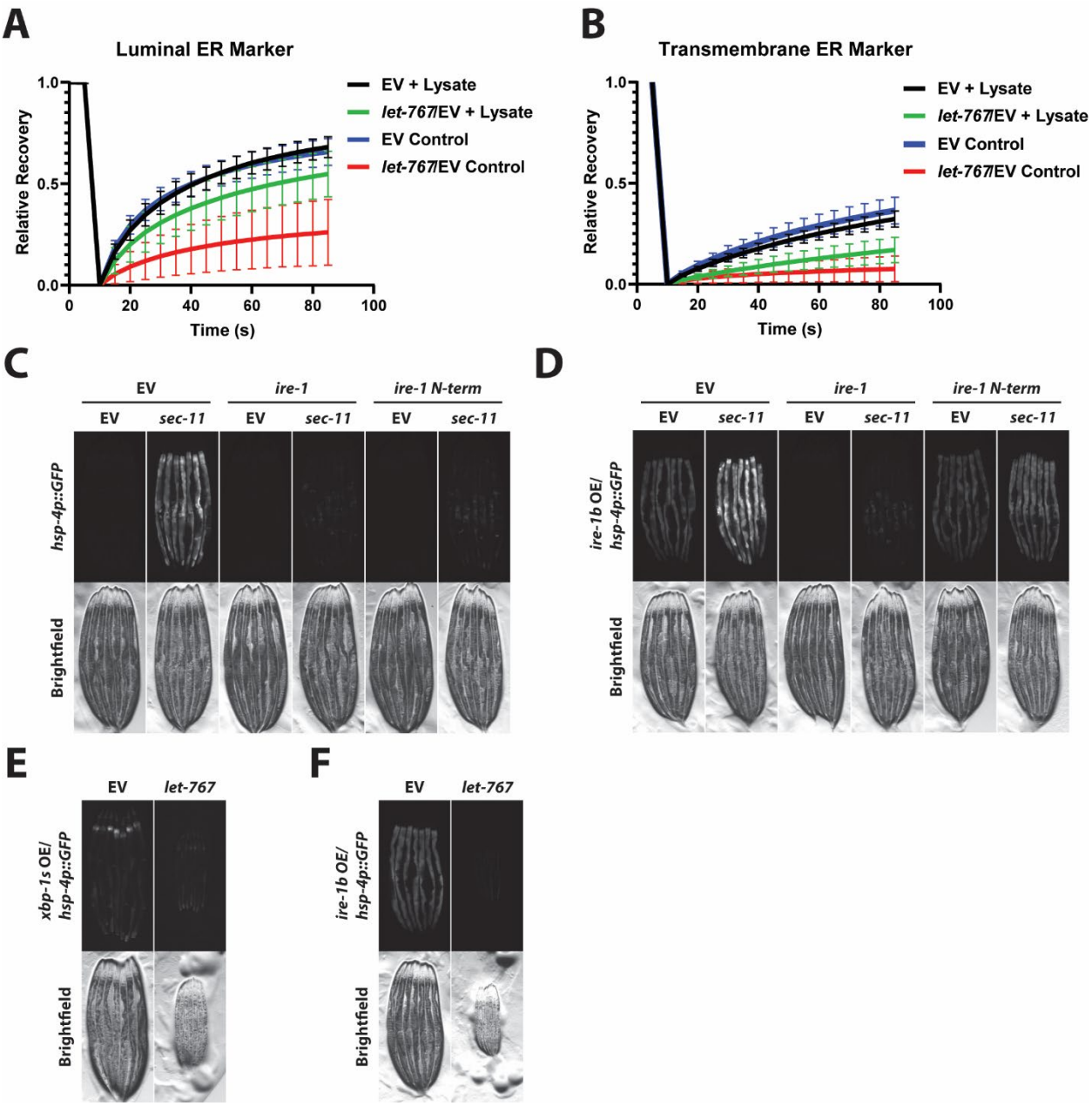

Figure 5. *let-767* mediated suppression of the UPR^{ER} through altered membrane dynamics

(A) FRAP analysis of intestinal *mRuby::HDEL* ER marker of animals (n = 20) grown on Empty Vector or 50% *let-767* RNAi supplemented with vehicle or crude lysate. (B) FRAP analysis of intestinal *GFP::C34B2.10* ER marker of animals (n = 20) grown on Empty Vector or 50% *let-767* RNAi supplemented with vehicle or crude lysate. (C) Transgenic animals expressing *hsp-4p::GFP* grown on Empty Vector or *sec-11* RNAi combined with Empty Vector, *ire-1*, or *ire-1* N-terminus RNAi to asses UPR^{ER} induction. (D) Transgenic animals expressing *hsp-4p::GFP* and intestinal *mRuby::ire-1b* grown on Empty Vector or *sec-11* RNAi combined with Empty Vector, *ire-1*, or *ire-1* N-terminus RNAi to asses UPR^{ER} induction. (E) Transgenic animals expressing *hsp-4p::GFP* and intestinal *xbp-1s* grown on Empty Vector or *let-767* RNAi to asses UPR^{ER} induction. (F) Transgenic animals expressing *hsp-4p::GFP* and intestinal *mRuby::ire-1b* grown on Empty Vector or *let-767* RNAi supplemented with vehicle or crude lysate to asses UPR^{ER} induction. All transcriptional reporter images contrast matched. Geometric mean ± SD are plotted on (A, B).

Figure 6. Model for *let-767* mediated suppression of the UPR^{ER}

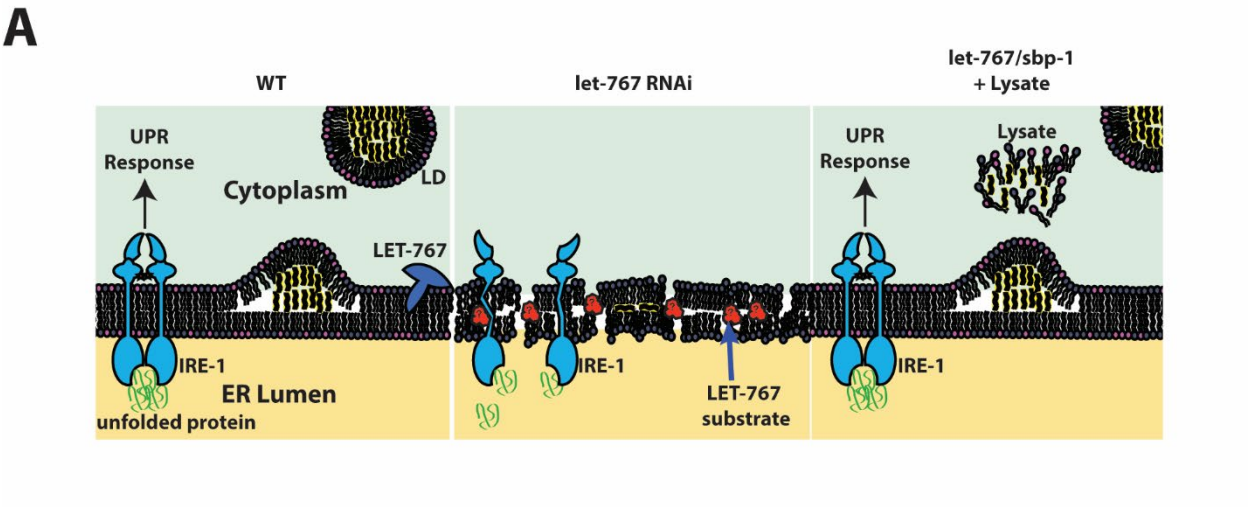

Figure 6. Model for *let-767* mediated suppression of the UPR^{ER}

(A) Under WT conditions, the ER produces lipids and lipid droplets, and responds to proteotoxic stress. *let-767* knockdown results in accumulation of its toxic substrate, resulting in reduced UPR^{ER} signaling and lipid synthesis. Knockdown of *sbp-1* to diminish lipid pathways upstream of *let-767* and supplementation of exogenous lipids restores ER signaling and lipid levels.

Chapter 4: Conclusions and Future Directions

4.1 Conclusions

We have identified the sterol dehydrogenase, *let-767*, as an essential gene for ER lipid and protein homeostasis. As a central hub for lipid synthesis and protein trafficking, the ER must be able to monitor and respond to imbalances in both to preserve cellular function. This feat is accomplished by the three branches of the UPR^{ER}, each capable of monitoring both misfolded proteins and ER membrane changes[5], [26], [75].

The ER must maintain lipid homeostasis in part, to preserve protein quality. The ER membrane composition must be controlled to provide environments that allow proper folding of transmembrane proteins, formation of transmembrane protein complexes, and translocation of nascent proteins [77]. Thus, it is no surprise that the UPR^{ER} responds to lipid changes that affect membrane quality such as phospholipid saturation and head group. Here, we find that knockdown of a steroid dehydrogenase, *let-767*, alters ER membrane qualities and global lipid metabolism, but does not instigate the UPR^{ER}.

Deficiencies in signaling and essential metabolites can often be compensated for by supplementation of the missing metabolites. For example, in *C. elegans*, addition of dafachronic acid or isoheptadecanoic acid to their food source prevents the phenotypes associated with mutations in those respective pathways. However, an inability to process metabolites can also result in toxic accumulation of metabolites, as in the cases of phenylketonuria or Zellweger syndrome, where phenylalanine or branched and very long chain fatty acids accumulate to toxic levels, respectively. In the case of *let-767* knockdown, we see phenotypes that fall into both categories. Knockdown animals require lipid supplementation of normal growth, but also loss of lipogenic pathways to rescue ER membrane signaling of the UPR^{ER}. Whether the accumulation of the LET-767 metabolite disrupts the ER enough to affect global lipid metabolism or whether the LET-767 product is in fact needed to promote lipid synthesis, remains unclear.

4.2 Future Directions

Changes in proteostasis contribute to aging, neurodegenerative disease, and metabolic disorders [9], [10]. While many of the major pathways monitoring proteostasis have been identified [5], we have yet to conclusively elucidate all the factors that impact these pathways. Our results bring to light the potential of the *let-767* lipid pathway to negatively regulate proteostasis response mechanisms. The ER is composed of many lipids, each with their own characteristics that can affect membrane quality. Previous work implicates *let-767* in both sterol and fatty acid metabolism; two lipid types known to affect membrane fluidity and function as signaling molecules [16], [62], [63]. Through biochemical analysis and further genetic screens, we may identify the specific lipid species and metabolic pathways of *let-767* which mediate influence over the UPR^{ER}.

Within our model, we propose that accumulation of a metabolite alters membrane dynamics and leads to impaired ER function. In cases of aging and obesity, we see drastic changes in lipid metabolism [31]. Understanding whether these metabolic changes also result in altered membrane dynamics would provide a potential mechanism through which age and obesity related diseases may progress. For example, the ability to induce the UPR^{ER} has been

shown to decline during the aging process. This has been partly ascribed to diminished *xbp-1* signaling [13], a potential downstream result of decreased membrane dynamics and perturbations in IRE-1 oligomerization comparable to those of *let-767* knockdown. Of interest, would be determining if any declines in membrane fluidity during the aging process are possibly due to reduced function of LET-767.

Increased UPR^{ER} signaling through ectopic expression of the activated form of *xbp-1*, *xbp-1s*, extends *C. elegans* lifespan and imbues increased proteotoxic stress survival [13]. During our investigation of *let-767*, we created a *C. elegans* strain ectopically expressing *ire-1b*, a possible isoform lacking the luminal unfolded protein sensing domain. While the luminal domain of IRE1 has been shown to be required for sensing proteotoxic stress and higher order oligomer formation, similarly truncated forms of IRE1have displayed increased basal UPR^{ER} and functional responsiveness to membrane lipid stress [25], [78], suggesting that the luminal domain is dispensable for some of its functions. In our hands, ectopic expression of *ire-1a* proved to be toxic, however, *ire-1b* animals appear phenotypically normal. Understanding how *ire-1b* signaling differs from *ire-1a* and whether it is also different from *xbp-1s* mediated activation of the UPR^{ER} would provide valuable insights on how chronic UPR^{ER} activation can contribute to both disease and lifespan extension.

Chapter 5: Appendix

5.1 Improved proteotoxic stress resistance through *ire-1* over-expression

ER homeostasis is monitored by three transmembrane proteins (IRE-1, PEK-1/PERK, ATF-6) capable of recognizing misfolded ER proteins and ER membrane disequilibrium. The most studied of these proteins, IRE-1, oligomerizes upon its activation and splices the *xbp-1* transcription factor mRNA to its more active isoform, *xbp-1s*. XPB-1S is then able to induce expression of key factors of the UPR^{ER} to restore ER homeostasis [5], [26], [27], [58]. Previous work has shown that ectopic activation of the UPR^{ER} through over-expression of *xbp-1s* can significantly improve survival of animals under proteotoxic stress and increase lifespan, likely through improved ER homeostasis [13]. Whether ectopic activation of the UPR^{ER} upstream of *xbp-1* has similar improvements on lifespan and stress resistance has not been thoroughly investigated.

We have demonstrated that intestinal over-expression of *ire-1* without the ER luminal domain (*ire-1b*) is sufficient to induce activation of the UPR^{ER} (Fig.5D). While the *ire-1* luminal domain has been shown to be required for clustering of mammalian IRE1 in response to proteotoxic stress, it is dispensable for lipid mediated activation of the UPR^{ER} [25], [78]. Interestingly, over-expression of the full *ire-1* (*ire-1a*) proved to be toxic during development (data not shown), implying a functional difference between UPR^{ER} induced by overexpression of *ire-1a* and *ire-1b*. Whether this difference is mechanistically distinct or a simply a difference in activation intensity remains to be determined; however, distinct functional outcomes between oligomeric states of *ire-1* have been previously reported [79].

Next, we tested whether over-expression of *ire-1b* is capable of increasing lifespan similar to *xbp-1s* over-expression. Our preliminary results suggest that *ire-1b* over-expression does not increase lifespan but is able to rescue the lifespan reduction caused by *xbp-1* RNAi (Fig.S1A). A possible explanation of these results is that the over-expression of *ire-1b* increases effective splicing of *xbp-1* to *xbp-1s* which is then able to compensate for the reduced levels of *xbp-1* mRNA caused by RNAi. Alternatively, increased IRE-1 functions independent of *xbp-1* splicing (*e.g.* regulated Ire1-dependent decay) may be responsible for the restored lifespan of *xbp-1* knockdown animals. Future lifespan analyses of *xbp-1* knockouts will provide insight on whether the rescued lifespan is independent of *xbp-1* splicing.

We then performed an ER stress survival analysis on *ire-1b* over-expressing (OE) animals. Our preliminary analysis showed that *ire-1b* over-expression did not improve ER stress resistance, similar to lifespans (Fig.S1B-C). However, these results were confounded by a ~66-70% censorship of *ire-1b* OE animals on tunicamycin treatment due to desiccation upon crawling up the sides of the plates (data not shown), compared to 15-18% censorship of N2 animals on tunicamycin. Further analysis will determine whether *ire-1b* over-expression may impart avoidance behaviors to animals undergoing ER stress. Interestingly, during the stress survival assay, we observed that a small percentage of eggs laid by *ire-1b* OE animals on tunicamycin treatment were able to develop to adulthood, while 100% of N2 animals hatching on tunicamycin died during early development (Fig.S1D). These results suggest that while *ire-1b*

over-expression may not increase lifespan or long-term tunicamycin stress resistance, it did protect animals from lethal tunicamycin stress during development.

Our preliminary results provide evidence that *ire-1* over-expression induces the UPR^{ER} in a manner distinct from previously described induction of the UPR^{ER} through *xbp-1s* over-expression [13]. While intestinal *ire-1b* OE animals did not display increases in lifespan or improved long-term ER stress resistance, *ire-1b* over-expression was nonetheless protective during development on tunicamycin induced ER stress. These contrasting results may be due to additional IRE-1 functions independent of *xbp-1* splicing. Furthermore, deletion of the *ire-1a* luminal domain was necessary to prevent lethal toxicity of *ire-1* over-expression. This further highlights the distinction between *xbp-1s* and *ire-1b* overexpression regarding activation of the UPR^{ER} and organismal health, as *xbp-1s* OE does not appear to be toxic. With further investigation, we hope to provide insight on the unique roles that *xbp-1* and *ire-1* play in determining whether induction of the UPR^{ER} is beneficial or detrimental to stress resistance and lifespan.

5.2 Appendix figures

Figure S1. Intestinal *ire-1b* over-expression does not increase lifespan, but improves development on tunicamycin

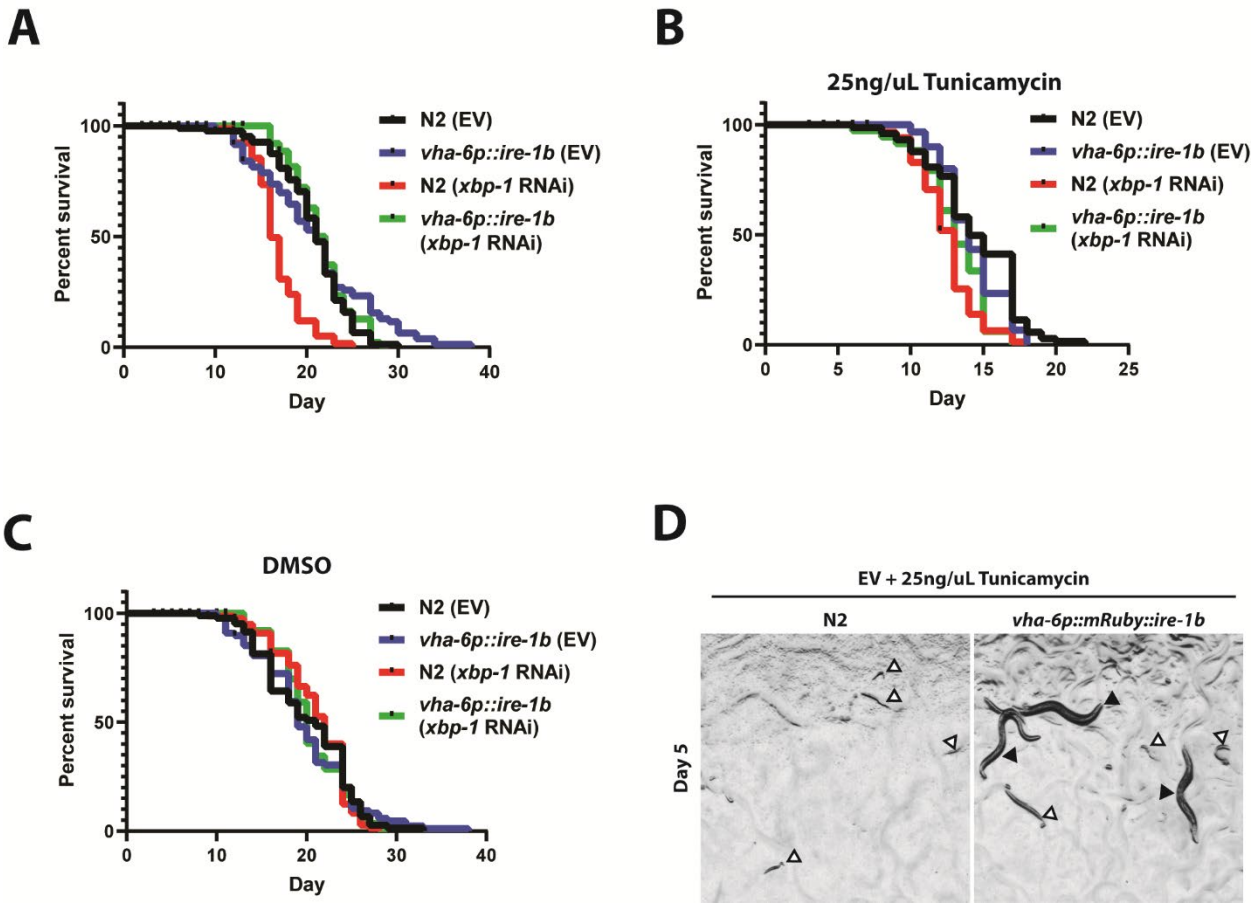

Figure S1. Intestinal *ire-1b* over-expression does not increase lifespan, but improves development on tunicamycin

(A) Lifespans of N2 or transgenic animals expressing *vha-6p::mRuby::ire-1b* grown on Empty Vector or *xbp-1* RNAi. (B-C) Concurrent survival assays of N2 or transgenic animals expressing *vha-6p::mRuby::ire-1b* transferred to ER stress conditions of 25ng/uL Tunicamycin (B) or control DMSO (C) conditions at day 1 of adulthood. Animals continuously grown on Empty Vector or *xbp-1* RNAi from L1 synchronization. (D) Day 5 N2 or transgenic animals expressing *vha-6p::mRuby::ire-1b* grown on Empty Vector with ER stress conditions of 25ng/uL Tunicamycin from hatch. White arrows denote dead animals. Black arrows denote animals developed to adults.

Chapter 6: References

[1] E. T. Powers, R. I. Morimoto, A. Dillin, J. W. Kelly, and W. E. Balch, "Biological and chemical approaches to diseases of proteostasis deficiency," *Annu. Rev. Biochem.*, vol. 78, pp. 959–991, 2009.

[2] Y. E. Kim, M. S. Hipp, A. Bracher, M. Hayer-Hartl, and F. U. Hartl, "Molecular Chaperone Functions in Protein Folding and Proteostasis," *Annu. Rev. Biochem.*, vol. 82, no. 1, pp. 323–355, 2013.

[3] R. Higuchi-Sanabria, P. A. Frankino, J. W. Paul, S. U. Tronnes, and A. Dillin, "A Futile Battle? Protein Quality Control and the Stress of Aging," *Dev. Cell*, vol. 44, no. 2, pp. 139–163, Jan. 2018.

[4] J. Hollien, J. H. Lin, H. Li, N. Stevens, P. Walter, and J. S. Weissman, "Regulated Ire1-dependent decay of messenger RNAs in mammalian cells," *J. Cell Biol.*, vol. 186, no. 3, pp. 323–331, Aug. 2009.

[5] C. J. Adams, M. C. Kopp, N. Larburu, P. R. Nowak, and M. M. U. Ali, "Structure and Molecular Mechanism of ER Stress Signaling by the Unfolded Protein Response Signal Activator IRE1," *Front. Mol. Biosci.*, vol. 6, Mar. 2019.

[6] C. Hetz, "The unfolded protein response: controlling cell fate decisions under ER stress and beyond," *Nat. Rev. Mol. Cell Biol.*, vol. 13, no. 2, pp. 89–102, Feb. 2012.

[7] N. T. Sprenkle, S. G. Sims, C. L. Sánchez, and G. P. Meares, "Endoplasmic reticulum stress and inflammation in the central nervous system," *Mol. Neurodegener.*, vol. 12, May 2017.

[8] N. Hamdan, P. Kritsiligkou, and C. M. Grant, "ER stress causes widespread protein aggregation and prion formation," *J. Cell Biol.*, vol. 216, no. 8, pp. 2295–2304, Aug. 2017.

[9] A. E. Frakes and A. Dillin, "The UPRER: Sensor and Coordinator of Organismal Homeostasis," *Mol. Cell*, vol. 66, no. 6, pp. 761–771, Jun. 2017.

[10] R. C. Taylor, "Aging and the UPR(ER)," *Brain Res.*, Apr. 2016.

[11] J. J. Yerbury *et al.*, "Walking the tightrope: proteostasis and neurodegenerative disease," *J. Neurochem.*, vol. 137, no. 4, pp. 489–505, May 2016.

[12] T. Shpilka and C. M. Haynes, "The mitochondrial UPR: mechanisms, physiological functions and implications in ageing," *Nat. Rev. Mol. Cell Biol.*, vol. 19, no. 2, pp. 109–120, Feb. 2018.

[13] R. C. Taylor and A. Dillin, "XBP-1 is a cell-nonautonomous regulator of stress resistance and longevity," *Cell*, vol. 153, no. 7, pp. 1435–1447, Jun. 2013.

[14] N. A. Baird *et al.*, "HSF-1 mediated cytoskeletal integrity determines thermotolerance and lifespan," *Science*, vol. 346, no. 6207, pp. 360–363, Oct. 2014.

[15] G. van Meer, D. R. Voelker, and G. W. Feigenson, "Membrane lipids: where they are and how they behave," *Nat. Rev. Mol. Cell Biol.*, vol. 9, no. 2, pp. 112–124, Feb. 2008.

[16] T. Harayama and H. Riezman, "Understanding the diversity of membrane lipid composition," *Nat. Rev. Mol. Cell Biol.*, vol. 19, no. 5, pp. 281–296, May 2018.

[17] J. A. Olzmann and P. Carvalho, "Dynamics and functions of lipid droplets," *Nat. Rev. Mol. Cell Biol.*, vol. 20, no. 3, p. 137, Mar. 2019.

[18] M. E. Ertunc and G. S. Hotamisligil, "Lipid signaling and lipotoxicity in metaflammation: indications for metabolic disease pathogenesis and treatment," *J. Lipid Res.*, vol. 57, no. 12, pp. 2099–2114, Dec. 2016.

[19] A. J. Kastaniotis *et al.*, "Mitochondrial fatty acid synthesis, fatty acids and mitochondrial physiology," *Biochim. Biophys. Acta Mol. Cell Biol. Lipids*, vol. 1862, no. 1, pp. 39–48, Jan. 2017.

[20] D. B. Jump, "Mammalian Fatty Acid Elongases," *Methods Mol. Biol. Clifton NJ*, vol. 579, pp. 375–389, 2009.

[21] I. J. Lodhi and C. F. Semenkovich, "Peroxisomes: a Nexus for Lipid Metabolism and Cellular Signaling," *Cell Metab.*, vol. 19, no. 3, pp. 380–392, Mar. 2014.

[22] P. Fagone and S. Jackowski, "Membrane phospholipid synthesis and endoplasmic reticulum function," *J. Lipid Res.*, vol. 50, no. Suppl, pp. S311–S316, Apr. 2009.

[23] Z. Song, A. M. Xiaoli, and F. Yang, “Regulation and Metabolic Significance of De Novo Lipogenesis in Adipose Tissues,” *Nutrients*, vol. 10, no. 10, Sep. 2018.
[24] H. Shimano and R. Sato, “SREBP-regulated lipid metabolism: convergent physiology — divergent pathophysiology,” *Nat. Rev. Endocrinol.*, vol. 13, no. 12, pp. 710–730, Dec. 2017.
[25] R. Volmer and D. Ron, “Lipid-dependent regulation of the unfolded protein response,” *Curr. Opin. Cell Biol.*, vol. 33, pp. 67–73, Apr. 2015.
[26] K. Halbleib *et al.*, “Activation of the Unfolded Protein Response by Lipid Bilayer Stress,” *Mol. Cell*, vol. 67, no. 4, pp. 673-684.e8, Aug. 2017.
[27] A. B. Tam *et al.*, “The UPR Activator ATF6 Responds to Proteotoxic and Lipotoxic Stress by Distinct Mechanisms,” *Dev. Cell*, vol. 46, no. 3, pp. 327-343.e7, Aug. 2018.
[28] N. Kawasaki, R. Asada, A. Saito, S. Kanemoto, and K. Imaizumi, “Obesity-induced endoplasmic reticulum stress causes chronic inflammation in adipose tissue,” *Sci. Rep.*, vol. 2, Nov. 2012.
[29] A. D. Garg, A. Kaczmarek, O. Krysko, P. Vandenabeele, D. V. Krysko, and P. Agostinis, “ER stress-induced inflammation: does it aid or impede disease progression?,” *Trends Mol. Med.*, vol. 18, no. 10, pp. 589–598, Oct. 2012.
[30] C. Contreras *et al.*, “Central Ceramide-Induced Hypothalamic Lipotoxicity and ER Stress Regulate Energy Balance,” *Cell Rep.*, vol. 9, no. 1, pp. 366–377, Sep. 2014.
[31] L. M. Pérez, H. Pareja-Galeano, F. Sanchis-Gomar, E. Emanuele, A. Lucia, and B. G. Gálvez, “‘Adipaging’: ageing and obesity share biological hallmarks related to a dysfunctional adipose tissue,” *J. Physiol.*, vol. 594, no. 12, pp. 3187–3207, Jun. 2016.
[32] D. J. Murphy, “The biogenesis and functions of lipid bodies in animals, plants and microorganisms,” *Prog. Lipid Res.*, vol. 40, no. 5, pp. 325–438, Sep. 2001.
[33] A. R. Kimmel and C. Sztalryd, “The Perilipins: Major Cytosolic Lipid Droplet-Associated Proteins and Their Roles in Cellular Lipid Storage, Mobilization, and Systemic Homeostasis,” *Annu. Rev. Nutr.*, vol. 36, pp. 471–509, Jul. 2016.
[34] A. S. Rambold, S. Cohen, and J. Lippincott-Schwartz, “Fatty Acid Trafficking in Starved Cells: Regulation by Lipid Droplet Lipolysis, Autophagy, and Mitochondrial Fusion Dynamics,” *Dev. Cell*, vol. 32, no. 6, pp. 678–692, Mar. 2015.
[35] J. K. Zehmer, Y. Huang, G. Peng, J. Pu, R. G. W. Anderson, and P. Liu, “A role for lipid droplets in inter-membrane lipid traffic,” *Proteomics*, vol. 9, no. 4, pp. 914–921, Feb. 2009.
[36] I. Y. Benador *et al.*, “Mitochondria Bound to Lipid Droplets Have Unique Bioenergetics, Composition, and Dynamics that Support Lipid Droplet Expansion,” *Cell Metab.*, vol. 27, no. 4, pp. 869-885.e6, Apr. 2018.
[37] T. Nolis, “Exploring the pathophysiology behind the more common genetic and acquired lipodystrophies,” *J. Hum. Genet.*, vol. 59, no. 1, pp. 16–23, Jan. 2014.
[38] S. Virtue and A. Vidal-Puig, “Adipose tissue expandability, lipotoxicity and the Metabolic Syndrome — An allostatic perspective,” *Biochim. Biophys. Acta BBA - Mol. Cell Biol. Lipids*, vol. 1801, no. 3, pp. 338–349, Mar. 2010.
[39] M. E. Hall, J. M. do Carmo, A. A. da Silva, L. A. Juncos, Z. Wang, and J. E. Hall, “Obesity, hypertension, and chronic kidney disease,” *Int. J. Nephrol. Renov. Dis.*, vol. 7, pp. 75–88, Feb. 2014.
[40] J.-P. Després and I. Lemieux, “Abdominal obesity and metabolic syndrome,” *Nature*, vol. 444, no. 7121, pp. 881–887, Dec. 2006.
[41] Y. Ding, Y. Wu, R. Zeng, and K. Liao, “Proteomic profiling of lipid droplet-associated proteins in primary adipocytes of normal and obese mouse,” *Acta Biochim. Biophys. Sin.*, vol. 44, no. 5, pp. 394–406, May 2012.
[42] M. D. Kristensen *et al.*, “Obesity leads to impairments in the morphology and organization of human skeletal muscle lipid droplets and mitochondrial networks, which are resolved with gastric bypass surgery-induced improvements in insulin sensitivity,” *Acta Physiol.*, vol. 0, no. ja, p. e13100.

[43] N. L. Gluchowski, M. Becuwe, T. C. Walther, and R. V. Farese Jr, “Lipid droplets and liver disease: from basic biology to clinical implications,” *Nat. Rev. Gastroenterol. Hepatol.*, vol. 14, no. 6, pp. 343–355, Jun. 2017.
[44] Ouimet Mireille and Marcel Yves L., “Regulation of Lipid Droplet Cholesterol Efflux From Macrophage Foam Cells,” *Arterioscler. Thromb. Vasc. Biol.*, vol. 32, no. 3, pp. 575–581, Mar. 2012.
[45] K. Bersuker and J. A. Olzmann, “Establishing the lipid droplet proteome: Mechanisms of lipid droplet protein targeting and degradation,” *Biochim. Biophys. Acta*, Jun. 2017.
[46] M. A. Welte, “Expanding Roles for Lipid Droplets,” *Curr. Biol. CB*, vol. 25, no. 11, pp. R470–R481, Jun. 2015.
[47] J. D. Vevea *et al.*, “Role for Lipid Droplet Biogenesis and Microlipophagy in Adaptation to Lipid Imbalance in Yeast,” *Dev. Cell*, vol. 35, no. 5, pp. 584–599, Jul. 2015.
[48] C. Zhang *et al.*, “Bacterial lipid droplets bind to DNA via an intermediary protein that enhances survival under stress,” *Nat. Commun.*, vol. 8, p. 15979, Jul. 2017.
[49] M. Ueno, W.-J. Shen, S. Patel, A. S. Greenberg, S. Azhar, and F. B. Kraemer, “Fat-specific protein 27 modulates nuclear factor of activated T cells 5 and the cellular response to stress,” *J. Lipid Res.*, vol. 54, no. 3, pp. 734–743, Mar. 2013.
[50] J. H. Lee *et al.*, “Lipid Droplet Protein LID-1 Mediates ATGL-1-Dependent Lipolysis during Fasting in Caenorhabditis elegans,” *Mol. Cell. Biol.*, vol. 34, no. 22, pp. 4165–4176, Nov. 2014.
[51] P. Narbonne and R. Roy, “Caenorhabditis elegans dauers need LKB1/AMPK to ration lipid reserves and ensure long-term survival,” *Nature*, vol. 457, no. 7226, pp. 210–214, Jan. 2009.
[52] A. P. Bailey *et al.*, “Antioxidant Role for Lipid Droplets in a Stem Cell Niche of Drosophila,” *Cell*, vol. 163, no. 2, pp. 340–353, Aug. 2015.
[53] L. Liu *et al.*, “Glial Lipid Droplets and ROS Induced by Mitochondrial Defects Promote Neurodegeneration,” *Cell*, vol. 160, no. 1–2, pp. 177–190, Jan. 2015.
[54] O. Moldavski *et al.*, “Lipid Droplets Are Essential for Efficient Clearance of Cytosolic Inclusion Bodies,” *Dev. Cell*, vol. 33, no. 5, pp. 603–610, Jun. 2015.
[55] C. Frøkjær-Jensen *et al.*, “Single copy insertion of transgenes in C. elegans,” *Nat. Genet.*, vol. 40, no. 11, pp. 1375–1383, Nov. 2008.
[56] R. Higuchi-Sanabria *et al.*, “Spatial regulation of the actin cytoskeleton by HSF-1 during aging,” *Mol. Biol. Cell*, vol. 29, no. 21, pp. 2522–2527, Oct. 2018.
[57] Y. Ding *et al.*, “Isolating lipid droplets from multiple species,” *Nat. Protoc.*, vol. 8, no. 1, pp. 43–51, Jan. 2013.
[58] X. Shen, R. E. Ellis, K. Sakaki, and R. J. Kaufman, “Genetic interactions due to constitutive and inducible gene regulation mediated by the unfolded protein response in C. elegans,” *PLoS Genet.*, vol. 1, no. 3, p. e37, Sep. 2005.
[59] P. Zhang *et al.*, “Proteomic Study and Marker Protein Identification of Caenorhabditis elegans Lipid Droplets,” *Mol. Cell. Proteomics*, vol. 11, no. 8, pp. 317–328, Aug. 2012.
[60] T. L. Vrablik, V. A. Petyuk, E. M. Larson, R. D. Smith, and J. L. Watts, “Lipidomic and proteomic analysis of Caenorhabditis elegans lipid droplets and identification of ACS-4 as a lipid droplet-associated protein,” *Biochim. Biophys. Acta BBA - Mol. Cell Biol. Lipids*, Jun. 2015.
[61] H. Na *et al.*, “Identification of lipid droplet structure-like/resident proteins in Caenorhabditis elegans,” *Biochim. Biophys. Acta BBA - Mol. Cell Res.*, May 2015.
[62] E. V. Entchev *et al.*, “LET-767 Is Required for the Production of Branched Chain and Long Chain Fatty Acids in Caenorhabditis elegans,” *J. Biol. Chem.*, vol. 283, no. 25, pp. 17550–17560, Jun. 2008.
[63] S. Desnoyers, P.-G. Blanchard, J.-F. St-Laurent, S. N. Gagnon, D. L. Baillie, and V. Luu-The, “Caenorhabditis elegans LET-767 is able to metabolize androgens and estrogens and likely shares common ancestor with human types 3 and 12 17β-hydroxysteroid dehydrogenases,” *J. Endocrinol.*, vol. 195, no. 2, pp. 271–279, Nov. 2007.

[64] L. M. Kuervers, C. L. Jones, N. J. O'Neil, and D. L. Baillie, "The sterol modifying enzyme LET-767 is essential for growth, reproduction and development in Caenorhabditis elegans," *Mol. Genet. Genomics*, vol. 270, no. 2, pp. 121–131, Oct. 2003.
[65] H. Zhang, N. Abraham, L. A. Khan, D. H. Hall, J. T. Fleming, and V. Göbel, "Apicobasal domain identities of expanding tubular membranes depend on glycosphingolipid biosynthesis," *Nat. Cell Biol.*, vol. 13, no. 10, pp. 1189–1201, Oct. 2011.
[66] S. Boland *et al.*, "Phosphorylated glycosphingolipids essential for cholesterol mobilization in *Caenorhabditis elegans*," *Nat. Chem. Biol.*, vol. 13, no. 6, pp. 647–654, Jun. 2017.
[67] M. Kniazeva, Q. T. Crawford, M. Seiber, C.-Y. Wang, and M. Han, "Monomethyl Branched-Chain Fatty Acids Play an Essential Role in Caenorhabditis elegans Development," *PLOS Biol.*, vol. 2, no. 9, p. e257, Aug. 2004.
[68] M. Kniazeva, T. Euler, and M. Han, "A branched-chain fatty acid is involved in post-embryonic growth control in parallel to the insulin receptor pathway and its biosynthesis is feedback-regulated in C. elegans," *Genes Dev.*, vol. 22, no. 15, pp. 2102–2110, Aug. 2008.
[69] D. Lee *et al.*, "SREBP and MDT-15 protect C. elegans from glucose-induced accelerated aging by preventing accumulation of saturated fat," *Genes Dev.*, vol. 29, no. 23, pp. 2490–2503, Dec. 2015.
[70] M. Kniazeva, H. Shen, T. Euler, C. Wang, and M. Han, "Regulation of maternal phospholipid composition and IP3-dependent embryonic membrane dynamics by a specific fatty acid metabolic event in C. elegans," *Genes Dev.*, vol. 26, no. 6, pp. 554–566, Mar. 2012.
[71] M. Ruiz *et al.*, "Membrane fluidity is regulated by the C. elegans transmembrane protein FLD-1 and its human homologs TLCD1/2," *eLife*, vol. 7, p. e40686, Dec. 2018.
[72] S. Zhang *et al.*, "Morphologically and Functionally Distinct Lipid Droplet Subpopulations," *Sci. Rep.*, vol. 6, p. 29539, Jul. 2016.
[73] K. Bersuker *et al.*, "A Proximity Labeling Strategy Provides Insights into the Composition and Dynamics of Lipid Droplet Proteomes," *Dev. Cell*, vol. 44, no. 1, pp. 97-112.e7, Jan. 2018.
[74] H. Zhang *et al.*, "Proteome of Skeletal Muscle Lipid Droplet Reveals Association with Mitochondria and Apolipoprotein A-I," *J. Proteome Res.*, vol. 10, no. 10, pp. 4757–4768, Oct. 2011.
[75] H. Zhu, H. Shen, A. K. Sewell, M. Kniazeva, and M. Han, "A novel sphingolipid-TORC1 pathway critically promotes postembryonic development in Caenorhabditis elegans," *eLife*, vol. 2, p. e00429, May 2013.
[76] F. Broué, P. Liere, C. Kenyon, and E.-E. Baulieu, "A steroid hormone that extends the lifespan of Caenorhabditis elegans," *Aging Cell*, vol. 6, no. 1, pp. 87–94, Feb. 2007.
[77] P. Shyu *et al.*, "Membrane phospholipid alteration causes chronic ER stress through early degradation of homeostatic ER-resident proteins," *Sci. Rep.*, vol. 9, no. 1, p. 8637, Jun. 2019.
[78] H. Li, A. V. Korennykh, S. L. Behrman, and P. Walter, "Mammalian endoplasmic reticulum stress sensor IRE1 signals by dynamic clustering," *Proc. Natl. Acad. Sci. U. S. A.*, vol. 107, no. 37, pp. 16113–16118, Sep. 2010.
[79] A. B. Tam, A. C. Koong, and M. Niwa, "Ire1 Has Distinct Catalytic Mechanisms for XBP1/HAC1 Splicing and RIDD," *Cell Rep.*, vol. 9, no. 3, pp. 850–858, Nov. 2014.